Sudden Death of Entanglement

Zeynepnur SAHINEL*
Ecole Polytechnique Fédérale de Lausanne
Quantum Science and Engineering Section

In this work, qubit disentanglement, decoherence and pairwise concurrence dynamics are investigated. The decoherence process is studied through a model consisting of stochastic fields to represent a realistic situation provided by Yu and Eberly [1]. The explicit derivation of the final density matrix of this stochastic model is obtained. For the pairwise concurrences, another model (Yönaç, [2]) consisting of two two-level atoms and uncoupled cavities is examined for different initial states and modes. Using numerical evaluations, how pairwise entanglements evolve and may exhibit entanglement sudden death (ESD) with periodic resurrection for each initial state condition is shown.

I. INTRODUCTION

Entanglement is critical not only for the transition between classical and quantum behavior but also for several key applications in quantum information. Protocols such as quantum cryptography, quantum teleportation, and superdense coding employ the entanglement phenomenon. Applications of interest, such as issues in quantum information processing (QIP), have prompted substantial research into quantum disentanglement control and entanglement dynamics. [3] In this work, both the disentanglement and the concurrence dynamics are studied in detail.

The paper is organized as follows. The two-qubit dephasing process using the stochastic model and Kraus operators are examined in Sec. II. Pairwise concurrences for two two-level atoms and uncoupled single-mode cavities model with explicit solutions and numerical analysis for partially entangled Bell states $|\Phi\rangle$ and $|\Psi\rangle$ are provided in Sec. III. This section investigates the one-photon single-mode cavities. Other initial states being more than one photon, coherent state and mixed states are studied in Secs. IV, V, VI, respectively. To comprehend the effect of the mode number of the cavity, the same model with two-modes cavity is investigated in Sec. VII. Finally, the obtained results and comments are given in Conclusion, Sec. VIII.

II. QUBIT DISENTANGLEMENT

This section investigates quantum disentanglement and decoherence via dephasing. The term decoherence has several interpretations in the literature. Disentanglement can be referred to as nonlocal or global decoherence. Whereas the local decoherence or local relaxation refers to the longitudinal and transverse decay of density matrix elements.[4] Quantum decoherence is characterized by the decay of the off-diagonal elements of the density matrix. In [1], the distinctions between the local and nonlocal decoherence are examined by employing a model consisting of two remote qubits and different noise sources. The model shown in Fig. (1) includes three different noise sources producing dephasing with different time scales to resemble a general practical situation. Two qubits A and B are coupled to a noisy environment both locally and collectively. This model can be described by the Hamiltonian:

$$H(t) = -\frac{1}{2}\mu\left[B(t)(\sigma_Z^A + \sigma_Z^B) + b_A(t)\sigma_Z^A + b_B(t)\sigma_Z^B\right] \tag{1}$$

where μ is the gyromagnetic ratio and $B(t)$, $b_A(t)$, $b_B(t)$ are stochastic environmental fluctuations imposed by Zeeman magnetic fields. The fields are assumed to be classical and statistically independent Markov processes satisfying:

$$\begin{aligned}
&\langle B(t)\rangle = 0\\
&\langle B(t)B(t')\rangle = \frac{\Gamma}{\mu^2}\delta(t-t')\\
&\langle b_i(t)\rangle = 0 \quad i = A, B\\
&\langle b_i(t)b_i(t')\rangle = \frac{\Gamma_i}{\mu^2}\delta(t-t')
\end{aligned} \tag{2}$$

where Γ and Γ_i are the damping rates due to the coupling to fluctuating magnetic fields. Expectation and the autocorrelations of the fields at different times are zero meaning that white-noise properties are satisfied, which also ensures the system undergoes a Markovian evolution. The dynamics of the Hamiltonian (1) can be described either by master equation [4] or Kraus operator-sum representation. For this model, the Kraus-model is employed. Yet, the derivation of these operators and the density operators are not given in [1]. Thus, in this paper explicit derivation of the final density matrix is given, and a comparison between this density matrix and the given Kraus sum is made.

$$U(t) = exp\left[-i\int_0^t H(t')dt'\right] \tag{3}$$

* zeynepnur.sahinel@epfl.ch

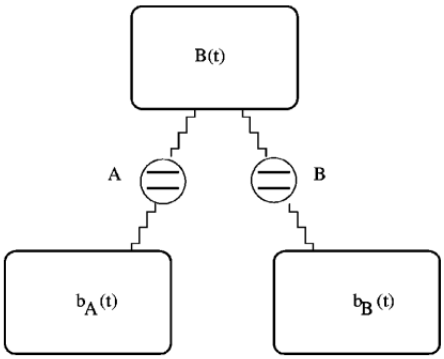

FIG. 1. The model consisting of two spin qubits A and B interacting with the stochastic magnetic field $B(t)$ and separately with the $b_A(t)$ and $b_B(t)$ [1]

Statistical density operator is given by:

$$\rho_{st}(t) = U(t)\rho(0)U^{\dagger}(t) \tag{4}$$

By calculating ensemble averages over the three noise fields $B(t)$, $b_A(t)$, and $b_B(t)$, it is possible to determine the density matrix for the two qubits:

$$\rho(t) = \langle\langle\langle\rho_{st}(t)\rangle\rangle\rangle \tag{5}$$

For the derivation firstly, the unitary operator is written in terms of the multiplication of the two terms belonging to the Hamiltonian.

$$\begin{aligned} U(t) =& exp\left[-i\left(-\frac{\mu}{2}\right)\int_0^t dt'[B(t')+b_A(t')]\sigma_Z^A\otimes I^B\right]\cdot \\ & exp\left[-i\left(-\frac{\mu}{2}\right)\int_0^t dt'[B(t')+b_B(t')]I^A\otimes\sigma_Z^B\right] \end{aligned} \tag{6}$$

Coefficients in front of the Pauli spin operators can be written as K and L:

$$\begin{aligned} K &= \left[\left(\frac{\mu}{2}\right)\int_0^t dt'[B(t')+b_A(t')\right] \\ L &= \left[\left(\frac{\mu}{2}\right)\int_0^t dt'[B(t')+b_B(t')\right] \end{aligned} \tag{7}$$

Thus, simplified version of the unitary operator:

$$U(t) = e^{iK\sigma_Z^A\otimes I^B}\cdot e^{iLI^A\otimes\sigma_Z^B} \tag{8}$$

where

$$\begin{aligned} e^{iK\sigma_Z^A\otimes I^B} &= \sum_{n=0}^{\infty}\frac{(iK)^n}{n!}(\sigma_Z^A\otimes I^B)^n \\ &= \sum_{n=0}^{\infty}\frac{(iK)^n}{n!}(\sigma_Z^A)^n\otimes(I^B)^n \\ &= e^{iK\sigma_Z^A}\otimes I^B \\ &= [\cos(K)I^A + i\sin(K)\sigma_Z^A]\otimes I^B \\ &= \begin{bmatrix} \cos(K)+i\sin(K) & 0 \\ 0 & cos(K)-i\sin(K)\end{bmatrix}\otimes\begin{bmatrix}1&0\\0&1\end{bmatrix} \\ &= \begin{bmatrix} e^{iK} & 0 & 0 & 0 \\ 0 & e^{iK} & 0 & 0 \\ 0 & 0 & e^{-iK} & 0 \\ 0 & 0 & 0 & e^{-iK}\end{bmatrix} \end{aligned} \tag{9}$$

Similarly, the second term in Eq. (8) can be written as:

$$e^{iLI^A\otimes\sigma_Z^B} = \begin{bmatrix} e^{iL} & 0 & 0 & 0 \\ 0 & e^{-iL} & 0 & 0 \\ 0 & 0 & e^{iL} & 0 \\ 0 & 0 & 0 & e^{-iL}\end{bmatrix} \tag{10}$$

Therefore, $U(t)$ becomes:

$$U(t) = \begin{bmatrix} e^{i(K+L)} & 0 & 0 & 0 \\ 0 & e^{i(K-L)} & 0 & 0 \\ 0 & 0 & e^{-i(K-L)} & 0 \\ 0 & 0 & 0 & e^{-i(K+L)}\end{bmatrix} \tag{11}$$

Using the Eq. (4), the statistical density operator can be found as:

$$\rho_{st}(t) = \begin{bmatrix} \rho_{11} & \rho_{12}e^{i2L} & \rho_{13}e^{i2K} & \rho_{14}e^{i2(K+L)} \\ \rho_{21}e^{-i2L} & \rho_{22} & \rho_{23}e^{i2(K-L)} & \rho_{24}e^{i2K} \\ \rho_{31}e^{-i2K} & \rho_{32}e^{-i2(K-L)} & \rho_{33} & \rho_{34}e^{i2L} \\ \rho_{41}e^{-i2(K+L)} & \rho_{42}e^{-i2K} & \rho_{43}e^{-i2L} & \rho_{44}\end{bmatrix}$$

While finding the ensemble averages over three noise fields, the characteristic function of the Gaussian Stochastic Process is employed.(12) Here, the noise fields are accepted as Gaussian.

$$\mathbb{E}[e^{i\int\beta(s)X(s)ds}] = e^{-\frac{1}{2}\iint\beta(s)C(s-s')\beta(s')dsds'} \tag{12}$$

where

$$\begin{aligned} \mathbb{E}[X(s)] =& 0, \\ \mathbb{E}[X(s)X(s')] =& C(s-s') \end{aligned} \tag{13}$$

For instance, the ensemble average of e^{i2L} can be expanded as below using Eq. (12), where L is given in Eq. (7).

$$\begin{aligned}\left\langle\left\langle\left\langle e^{i2L}\right\rangle\right\rangle\right\rangle &= e^{i\int_0^t \mu B(t')dt'}\cdot e^{i\int_0^t \mu b_B(t')dt'} \\ &= e^{-\frac{1}{2}\int_0^t\int \mu\left\langle B(t)B(t')\right\rangle\mu dtdt'}\cdot e^{-\frac{1}{2}\int_0^t\int \mu\left\langle b_B(t)b_B(t')\right\rangle\mu dtdt'}\end{aligned} \tag{14}$$

where $X(s)$ and $C(s-s')$ become μ and $\langle B(t)B(t')\rangle$. From the given autocorrelations relations in Eq. (2),

$$\begin{aligned}e^{-\frac{1}{2}\int_0^t\int \mu\left\langle B(t)B(t')\right\rangle\mu dtdt'} &= e^{-\frac{1}{2}\mu^2\frac{\Gamma}{\mu^2}\int_0^t\int \delta(t-t')dtdt'} \\ &= e^{-\frac{1}{2}\Gamma t}\end{aligned}$$

$$\begin{aligned}e^{-\frac{1}{2}\int_0^t\int \mu\left\langle b_B(t)b_B(t')\right\rangle\mu dtdt'} &= e^{-\frac{1}{2}\mu^2\frac{\Gamma_B}{\mu^2}\int_0^t\int \delta(t-t')dtdt'} \\ &= e^{-\frac{1}{2}\Gamma_B t}\end{aligned}$$

$$\left\langle\left\langle\left\langle e^{i2L}\right\rangle\right\rangle\right\rangle = e^{-\frac{(\Gamma+\Gamma_B)t}{2}} \tag{15}$$

Eq. 15 shows the final ensemble average over three noise fields $B(t), b_A(t), b_B(t)$. A similar process can be applied to the other matrix elements of the statistical density operator. Thus final density matrix $\rho(t)$ is given below.

$$\begin{bmatrix} \rho_{11} & \rho_{12}e^{-\frac{(\Gamma+\Gamma_B)t}{2}} & \rho_{13}e^{-\frac{(\Gamma+\Gamma_A)t}{2}} & \rho_{14}e^{-\frac{(\Gamma_A+\Gamma_B+4\Gamma)t}{2}} \\ \rho_{21}e^{-\frac{(\Gamma+\Gamma_B)t}{2}} & \rho_{22} & \rho_{23}e^{-\frac{(\Gamma_A+\Gamma_B)t}{2}} & \rho_{24}e^{-\frac{(\Gamma+\Gamma_A)t}{2}} \\ \rho_{31}e^{-\frac{(\Gamma+\Gamma_A)t}{2}} & \rho_{32}e^{-\frac{(\Gamma_A+\Gamma_B)t}{2}} & \rho_{33} & \rho_{34}e^{-\frac{(\Gamma+\Gamma_B)t}{2}} \\ \rho_{41}e^{-\frac{(\Gamma_A+\Gamma_B+4\Gamma)t}{2}} & \rho_{42}e^{-\frac{(\Gamma+\Gamma_A)t}{2}} & \rho_{43}e^{-\frac{(\Gamma+\Gamma_B)t}{2}} & \rho_{44} \end{bmatrix} \tag{16}$$

In the article [1], the decoherence process is described via the quantum channels. Let ε be a quantum channel which maps the input state $\rho(0)$ to a final state $\rho(t)$. The action of this map can be defined by Kraus operators K_μ.

$$\rho(t) = \varepsilon(\rho) = \sum_{\mu=1}^{N} K_\mu^\dagger(t)\rho(0)K_\mu(t) \tag{17}$$

Kraus operator K_μ is not unique and they have to satisfy

$$\sum_\mu K_\mu^\dagger K_\mu = I \tag{18}$$

for all time t. The solution for the Eq. (5) is described in terms of 12 Kraus operators.

$$\rho(t) = \varepsilon(\rho(0)) = \sum_{i,j=1}^{2}\sum_{k=1}^{3} D_k^\dagger E_j^\dagger F_i^\dagger \rho(0) F_i E_j D_k \tag{19}$$

where the Krauss operators for the local interaction between $b_A(t)$ and $b_B(t)$ are given by

$$E_1 = \begin{bmatrix} 1 & 0 \\ 0 & \gamma_A(t) \end{bmatrix}\otimes I, \quad E_2 = \begin{bmatrix} 0 & 0 \\ 0 & \omega_A(t) \end{bmatrix}\otimes I \tag{20}$$

$$F_1 = I\otimes\begin{bmatrix} 1 & 0 \\ 0 & \gamma_B(t) \end{bmatrix}, \quad F_2 = I\otimes\begin{bmatrix} 0 & 0 \\ 0 & \omega_B(t) \end{bmatrix} \tag{21}$$

and the Kraus operators for the collective interaction with $B(t)$ are given by

$$\begin{aligned} D_1 &= \begin{bmatrix} \gamma(t) & 0 & 0 & 0 \\ 0 & 1 & 0 & 0 \\ 0 & 0 & 1 & 0 \\ 0 & 0 & 0 & \gamma(t) \end{bmatrix}, \\ D_2 &= \begin{bmatrix} \omega_1(t) & 0 & 0 & 0 \\ 0 & 0 & 0 & 0 \\ 0 & 0 & 0 & 0 \\ 0 & 0 & 0 & \omega_2(t) \end{bmatrix}, \\ D_3 &= \begin{bmatrix} 0 & 0 & 0 & 0 \\ 0 & 0 & 0 & 0 \\ 0 & 0 & 0 & 0 \\ 0 & 0 & 0 & \omega_3(t) \end{bmatrix} \end{aligned} \tag{22}$$

The parameters appearing above is given by:

$$\begin{aligned} &\gamma_A(t) = e^{-t/2T_2^A}, \quad \gamma_B(t) = e^{-t/2T_2^B}, \\ &\omega_A(t) = \sqrt{1-e^{-t/2T_2^A}}, \quad \omega_B(t) = \sqrt{1-e^{-t/2T_2^B}}, \\ &\gamma(t) = e^{-t/2T_2}, \quad \omega_1(t) = \sqrt{1-e^{-t/T_2}}, \\ &\omega_2(t) = -e^{-t/T_2}\sqrt{1-e^{-t/T_2}}, \\ &\omega_3(t) = \sqrt{(1-e^{-t/2T_2})(1-e^{-2t/T_2})} \end{aligned} \tag{23}$$

where $T_2 = 1/\Gamma$ is the phase relaxation time because of the collective interaction with $B(t)$. Likewise $T_2^A = 1/\Gamma_A$ and $T_2^B = 1/\Gamma_B$ are the phase relaxation times due to the local interaction with $b_A(t)$ and $b_B(t)$ respectively.

Applying, the Kraus operators above, one can achive the density matrix shown in Eq. (16). Later subsections of this section are summarized version of the results given in [1].

A. Two-qubit local dephasing channel

When the qubits only interact with local magnetic fields $b_A(t)$ and $b_B(t)$, then the channel ε_{AB} can be described with 4 Kraus operators being:

$$M_1 = E_1F_1, \quad M_2 = E_1F_2$$
$$M_3 = E_2F_1, \quad M_4 = E_2F_2 \tag{24}$$

where E and F operators are defined in Eqs. (20) and (21).Thus, the effect of ε_{AB} can be shown as:

$$\rho(t) = \varepsilon_{AB}(\rho(0)) = \sum_{\mu=1}^{4} M_\mu^\dagger \rho(0) M_\mu \tag{25}$$

$$\begin{bmatrix} \rho_{11} & \gamma_B\rho_{12} & \gamma_A\rho_{13} & \gamma_A\gamma_B\rho_{14} \\ \gamma_B\rho_{21} & \rho_{22} & \gamma_A\gamma_B\rho_{23} & \gamma_A\rho_{24} \\ \gamma_A\rho_{31} & \gamma_A\gamma_B\rho_{32} & \rho_{33} & \gamma_B\rho_{34} \\ \gamma_A\gamma_B\rho_{41} & \gamma_A\rho_{42} & \gamma_B\rho_{43} & \rho_{44} \end{bmatrix} \tag{26}$$

Since $B(t) = 0$, one can say that the $\Gamma = 0$. Thus, putting this result into consideration, this matrix (26) can directly be obtained from the final density matrix (16). Here, γ_A and γ_B are defined in Eq. (23) which are time dependent. This channel affects all the matrix elements except the diagonal ones. Similar to this procedure, the effects of one-qubit local dephasing channels ε_A and ε_B can be described.

B. Local and Mixed Dephasing

The local dephasing rate of the qubit can be written as reduced density matrices obtained from the density matrix (26):

$$s^A = Tr_B[\rho] \quad s^B = Tr_A[\rho] \tag{27}$$

Thus, the reduced density matrices:

$$s^A(t) = \begin{bmatrix} \rho_{11}(t) + \rho_{22}(t) & \rho_{13}(t) + \rho_{24}(t) \\ \rho_{31}(t) + \rho_{42}(t) & \rho_{33}(t) + \rho_{44}(t) \end{bmatrix} \tag{28}$$

$$s^B(t) = \begin{bmatrix} \rho_{11}(t) + \rho_{33}(t) & \rho_{12}(t) + \rho_{34}(t) \\ \rho_{21}(t) + \rho_{43}(t) & \rho_{22}(t) + \rho_{44}(t) \end{bmatrix} \tag{29}$$

The dephasing rates are determined by the off-diagonal elements:

$$s_{12}^A = \rho_{13}(t) + \rho_{24}(t) = \gamma_A s_{12}^A(0) \tag{30}$$
$$s_{12}^B = \rho_{12}(t) + \rho_{34}(t) = \gamma_B s_{12}^B(0) \tag{31}$$

Thus the dephasing times τ_A and τ_B can be found as using $\gamma_A(t)$ (23):

$$\tau_A = 2T_2^A = \frac{2}{\Gamma_A} \quad \tau_B = \frac{2}{\Gamma_B} \tag{32}$$

Likewise in the local dephasing process, the decoherence rate for the composite system can be described by the off-diagonal elements of the density matrix (26). The off-diagonal elements:

$$\rho_{ij}(t) = e^{\Gamma_{ij}t}\rho_{ij}(0) \tag{33}$$

Thus,

$$\tau_{dec} = \frac{1}{\Gamma_{ij}} \tag{34}$$

where,

$$\Gamma_{12} = \Gamma_{34} = \frac{\Gamma_B}{2}, \tag{35}$$
$$\Gamma_{13} = \Gamma_{24} = \frac{\Gamma_A}{2}, \tag{36}$$
$$\Gamma_{14} = \Gamma_{23} = \frac{\Gamma_A + \Gamma_B}{2} \tag{37}$$

The corresponding decoherence rate $1/\tau$ is defined as mixed dephasing rate. The mixed dephasing rate is determined by the slower decaying elements, and in general

$$\tau >> \tau_A, \tau_B \tag{38}$$

C. Entanglement Decay

The amount of the entanglement should be measured to describe the dynamics of the entanglement. Since the entanglement decoherences are typically related to mixed states, Wootter's concurrence [5] is employed in [1]. The concurrence varies from 0 to 1 where 0 and 1 represent the product state and the maximally entangled state respectively. For two qubits, the concurrence can be calculated from the density matrix:

$$C(\rho) = max(0, \sqrt{\lambda_1}, \sqrt{\lambda_2}, \sqrt{\lambda_3}, \sqrt{\lambda_4}) \tag{39}$$

where the λ_is are the eigenvalues of the matrix:

$$\varrho = \rho(\sigma_y^A \otimes \sigma_y^B)\rho^*(\sigma_y^A \otimes \sigma_y^B) \tag{40}$$

1. Entanglement decay under two-qubit dephasing channel

It is found that all entangled states decay at rates that are faster than the dephasing rates of an individual qubit [1]. To prove that Jensen's Inequality is used:

$$C\left(\sum_{\mu=1}^{n} p_\mu \rho_\mu\right) \leq \sum_{\mu=1}^{n} p_\mu C(\rho_\mu) \tag{41}$$

where $C(\rho)$ is a convex function. Applying the above inequality to Eq. (25):

$$C(\rho(t)) \leq \sum_{\mu=1}^{4} C\left(M_\mu^\dagger \rho(0) M_\mu\right) \tag{42}$$

For further simplification, ρ_{out} term can be introduced:

$$\rho_{out} = M_\mu^\dagger \rho(0) M_\mu \tag{43}$$

Substituting ρ_{out} into Eq. (40):

$$\begin{aligned} \varrho &= \rho_{out}(\sigma_y^A \otimes \sigma_y^B)\rho_{out}^*(\sigma_y^A \otimes \sigma_y^B) \\ &= M_\mu^\dagger \rho M_\mu (\sigma_y^A \otimes \sigma_y^B) M_\mu^T \rho^* M_\mu^* (\sigma_y^A \otimes \sigma_y^B) \end{aligned} \tag{44}$$

Since M_μ and $M_\mu^\dagger$ matrices are diagonal the above equation can be written as:

$$\varrho = \rho M_\mu (\sigma_y^A \otimes \sigma_y^B) M_\mu^T \rho^* M_\mu^* (\sigma_y^A \otimes \sigma_y^B) M_\mu^\dagger \tag{45}$$

Moreover the Kraus operators are given in Eq. (20) satisfy the $M_\mu^T = M_\mu^\dagger = M_\mu^*$. Thus,

$$M_\mu (\sigma_y^A \otimes \sigma_y^B) M_\mu = \begin{cases} \gamma_A \gamma_B (\sigma_y^A \otimes \sigma_y^B), & \text{if } \mu = 1 \\ 0 & \text{if } \mu \neq 1 \end{cases} \tag{46}$$

Then Eq. (45) becomes:

$$\varrho = \begin{cases} \gamma_A^2 \gamma_B^2 \rho (\sigma_y^A \otimes \sigma_y^B) \rho^* (\sigma_y^A \otimes \sigma_y^B), & \text{if } \mu = 1 \\ 0 & \text{if } \mu \neq 1 \end{cases} \tag{47}$$

Using the concurrence definition given in Eq. (40) and the inequality (42):

$$C(\rho(t)) \leq \gamma_A \gamma_B C(\rho(0)) \tag{48}$$

Thus, the entanglement decay time τ_e can be written as:

$$\frac{1}{\tau_e} = \frac{1}{\tau_A} + \frac{1}{\tau_B} \tag{49}$$

From this result, it can be said that the entanglement decay time for the two-qubit channel is shorter than the local dephasing times τ_A and τ_B and therefore shorter than the mixed dephasing time τ (38).

FIG. 2. A schematic diagram of the double JC model in which there is no communication between the cavities [6]

2. Entanglement decay under one-qubit dephasing channel

With the same procedure followed in the entanglement decay under two-qubit channel, the effect of the one-qubit channel can be found as:

$$C(\varepsilon_A(\rho(0))) \leq \gamma_A C(\rho(0)) \tag{50}$$

$$C(\varepsilon_B(\rho(0))) \leq \gamma_B C(\rho(0)) \tag{51}$$

One-qubit local dephasing channels can completely destroy the quantum entanglement after the dephasing times τ_A and τ_B. Whereas, in general, one-qubit channels can not destroy the coherence of the two-qubit composite system.

III. PAIRWISE CONCURRENCE DYNAMICS

This section examines two time-evolving quantum systems that have no interaction, and whose mutual entanglement evolves in an unprecedented way compared to previous section.[2, 6] This system consists of two two-level atoms, each in single-mode near-resonant cavities. (Fig. 2). This model is called as double Jaynes-Cummings (JC). Before investigating the double JC model, one should introduce the JC model for one atom in a single-mode cavity. [7]

$$\hat{H} = \hat{H}_{cavity} + \hat{H}_{atom} + \hat{H}_{interaction} \tag{52}$$

$$\hat{H} = \hbar\omega \hat{a}^\dagger \hat{a} + \frac{1}{2}\hbar\omega_A \sigma_z + \hbar g(\hat{a}\sigma_+ + \hat{a}^\dagger \sigma_-) \tag{53}$$

Here the cavity is modelled as quantum harmonic oscillator. The Hamiltonian is a $\infty \times \infty$ matrix in a Block structure. One needs to find invariant subspaces. For this purpose, a new operator called number of excitations $\hat{N}_{exc}$ is introduced:

$$\hat{N}_{exc} = \hat{a}^\dagger \hat{a} + \sigma_+ \sigma_- \tag{54}$$

$$\hat{N}_{exc} |g, n\rangle = n |g, n\rangle \tag{55}$$

$$\hat{N}_{exc} |e, n-1\rangle = n |e, n-1\rangle \tag{56}$$

where $|g, n\rangle$ and $|e, n-1\rangle$ are the eigenstates of the $\hat{N}_{exc}$ with the eigenvalue n. e and g refer to the excited and the ground state respectively. Here, n represents the

number of photons. Since the $\hat{N}_{exc}$ and the Hamiltonian commutes, the JC Hamiltonian has the same eigenstates with $\hat{N}_{exc}$. Thus, the Hamiltonian can be written as:

$$\hat{H}\begin{pmatrix}|g,n\rangle\\|e,n-1\rangle\end{pmatrix}=\hbar\begin{pmatrix}-\frac{\omega_A}{2}+\omega n & g\sqrt{n}\\ g\sqrt{n} & \frac{\omega_A}{2}+\omega n\end{pmatrix}\begin{pmatrix}|g,n\rangle\\|e,n-1\rangle\end{pmatrix} \tag{57}$$

By diagonalizing this Hamiltonian matrix, the eigenvalue can be obtained:

$$\lambda_n^{\pm}=n\omega+\frac{1}{2}(\Delta\pm\sqrt{\Delta^2+G_n^2}) \tag{58}$$

where $\Delta=\omega-\omega_A$ is detuning, $G_n=2g\sqrt{n}$ is the n-photon Rabi frequency. The corresponding eigenstates are:

$$|\psi_0\rangle=|g,0\rangle \tag{59}$$
$$|\psi_n^+\rangle=c_n|e,n-1\rangle+s_n|g,n\rangle \tag{60}$$
$$|\psi_n^-\rangle=-s_n|e,n-1\rangle+c_n|g,n\rangle \tag{61}$$
$$c_n=\cos\left(\frac{\Theta_n}{2}\right)\quad s_n=\sin\left(\frac{\Theta_n}{2}\right) \tag{62}$$

where,

$$\cos(\Theta_n)=\frac{\Delta}{\sqrt{\Delta^2+G_n^2}}\quad \sin(\Theta_n)=\frac{G_n}{\sqrt{\Delta^2+G_n^2}} \tag{63}$$

These eigenstates are called dressed-atom states. The unperturbed atomic eigenstates $|g\rangle$, $|e\rangle$ are modified (dressed) by the interaction with the cavity field. And their eigenfrequencies are shifted by an amount determined by the coupling strength g, which is a Stark effect. [8] Even if no photon is present in the cavity, there will be a level splitting, the vacuum Rabi splitting 2g between the exact eigenstates of the combined atom-cavity system. (see Fig. 3)

The JC model explained above can be employed for the doubled system with the Hamiltonian:

$$\begin{aligned}H_{tot}=&\omega\hat{a}^\dagger\hat{a}+\frac{\omega_0}{2}\sigma_z^A+g(\hat{a}^\dagger\sigma_-^A+\hat{a}\sigma_+^A)+\\&\omega\hat{b}^\dagger\hat{b}+\frac{\omega_0}{2}\sigma_z^B+g(\hat{b}^\dagger\sigma_-^B+\hat{b}\sigma_+^B)\end{aligned} \tag{64}$$

where ω_0 is the frequency of atom and ω is the frequency of the cavity. (with $\hbar=1$) And A and B represent the atom A and B respectively. Similarly $\hat{a}$ and $\hat{b}$ correspond to cavity a and cavity b shown in Fig. (2). The eigenstates of this Hamiltonian (64) are products of the dressed states of the separate JC systems. For either system Aa or Bb, Hamiltonian can be written as:

$$H_{JC}|\psi_n^{\pm}\rangle=\lambda_n^{\pm}|\psi_n^{\pm}\rangle \tag{65}$$

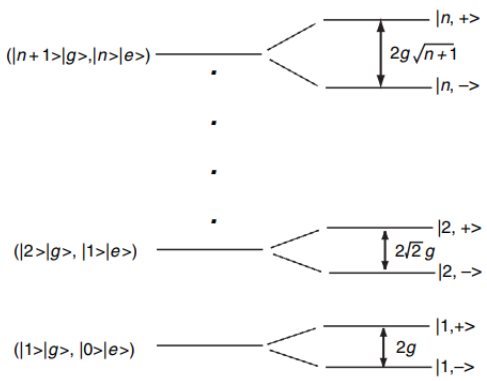

FIG. 3. The dressed states for the energy eigenstates of the Jaynes–Cummings interaction. The degenerate states for zero interaction are shown on the left. When the interaction is activated the degeneracies are lifted, shown on the right [7, Chapter 10]

In this section, we are only dealing with 1 photon inside the cavity. In [2], two groups of pure initial states which are super-positions of the Bell States:

$$|\Phi_{AB}\rangle=\cos(\alpha)|e_A,e_B\rangle+\sin(\alpha)|g_A,g_B\rangle \tag{66}$$
$$|\Psi_{AB}\rangle=\cos(\alpha)|e_A,g_B\rangle+\sin(\alpha)|g_A,e_B\rangle \tag{67}$$

are examined. In this paper, the explicit derivations are made for concurrences of these initial partially entangled Bell states. For the entanglement measurement, the Wootter concurrence is employed similar to Section (II). Where the concurrence C is less than 1 and greater than 0. $C=0$ indicates zero entanglement whereas, $C=1$ means maximally pure state entanglement. This double JC model can be treated as a four-qubit model. All reductions to two-qubit form are obtained by tracing over the other two qubits yielding a two-qubit mixed state always having the X form:

$$\rho=\begin{bmatrix}a&0&0&w\\0&b&z&0\\0&z^*&c&0\\w^*&0&0&d\end{bmatrix} \tag{68}$$

The concurrence of this mixed state can be found using the procedure followed in Section (II) Wootter's concurrence calculation:

$$C=2max[0,|z|-\sqrt{ad},|w|-\sqrt{bc}]=max[0,Q(t)] \tag{69}$$

For the bipartite entanglement, six different concurrences occur being C_{AB}, C_{ab}, C_{Ab}, C_{aB}, C_{Aa}, C_{Bb}. Except C_{Aa}, C_{Bb}, all remaining concurrences are the remote entanglements. Q is an important term when expressing conservation relations. In some cases, Q can be negative, unlike C.

A. Partially Entangled Bell State $|\Phi_{AB}\rangle$

$$|\Phi(0)\rangle = |\Phi_{AB}\rangle \otimes |0_a, 0_b\rangle \tag{70}$$

$$|\Phi(0)\rangle = (\cos(\alpha)\,|e_A, e_B\rangle + \sin(\alpha)\,|g_A, g_B\rangle) \otimes |0_a, 0_b\rangle \tag{71}$$

$$|\Phi(0)\rangle = \cos(\alpha)\,|e_A, 0_a\rangle \otimes |e_B, 0_b\rangle + \sin(\alpha)\,|g_A, 0_a\rangle \otimes |g_B, 0_b\rangle \tag{72}$$

One can write the initial state of the system in terms of the dressed states. For the one photon case, the dressed states become:

$$|\Psi_0\rangle = |g, 0\rangle \tag{73}$$

$$|\Psi_1^+\rangle = \cos\left(\frac{\Theta}{2}\right)|e, 0\rangle + \sin\left(\frac{\Theta}{2}\right)|g, 1\rangle \tag{74}$$

$$|\Psi_1^-\rangle = -\sin\left(\frac{\Theta}{2}\right)|e, 0\rangle + \cos\left(\frac{\Theta}{2}\right)|g, 1\rangle \tag{75}$$

$$|e_A, 0_a\rangle = c\,|\Psi_1^+\rangle - s\,|\Psi_1^-\rangle \tag{76}$$

$$|g_A, 1_a\rangle = s\,|\Psi_1^+\rangle + c\,|\Psi_1^-\rangle \tag{77}$$

$$|g_A, 0_a\rangle = |\Psi_0\rangle \tag{78}$$

Using these dressed states, the given initial Bell state can be written as below where c and s stand for $\cos\left(\frac{\Theta}{2}\right)$ and $\sin\left(\frac{\Theta}{2}\right)$ respectively:

$$|\Phi(0)\rangle = \cos(\alpha)(c\,|\Psi_1^+\rangle_A - s\,|\Psi_1^-\rangle_A) \otimes (c\,|\Psi_1^+\rangle_B \tag{79}$$

$$- s\,|\Psi_1^-\rangle_B) + \sin(\alpha)\,|\Psi_0\rangle_A \otimes |\Psi_0\rangle_B \tag{80}$$

From the Schrodinger Equation:

$$|\Phi^{\pm}(t)\rangle = e^{-i\lambda^{\pm}t}\,|\Phi^{\pm}(0)\rangle \tag{81}$$

Thus the wave function at t becomes:

$$\begin{aligned}|\Phi(t)\rangle =& \cos(\alpha)(ce^{-i\lambda^+t}\,|\Psi_1^+\rangle_A - se^{-i\lambda^-t}\,|\Psi_1^-\rangle_A) \otimes \\ & (ce^{-i\lambda^+t}\,|\Psi_1^+\rangle_B - se^{-i\lambda^-t}\,|\Psi_1^-\rangle_B) + \\ & \sin(\alpha)\,|\Psi_0\rangle_A \otimes |\Psi_0\rangle_B\end{aligned} \tag{82}$$

To take partial trace over individual atoms or cavities, one need to revert to the bare bases. Inserting the Eqs. (73), (74), (75):

$$\begin{aligned}|\Phi(t)\rangle =& \cos(\alpha)\left[(c^2e^{-i\lambda^+t} + s^2e^{-i\lambda^-t})\,|e_A, 0_a\rangle + \right. \\ & \left.(cse^{-i\lambda^+t} - cse^{-i\lambda^-t})\,|g_A, 0_a\rangle\right] \otimes \\ & \left[(c^2e^{-i\lambda^+t} + s^2e^{-i\lambda^-t})\,|e_B, 0_b\rangle + \right. \\ & \left.(cse^{-i\lambda^+t} - cse^{i\lambda^-t})\,|g_B, 0_b\rangle\right] + \\ & \sin(\alpha)\,|g_A, 0_a\rangle \otimes |g_B, 0_b\rangle\end{aligned} \tag{83}$$

The Eq. (83) can be simplified using the coefficients below:

$$\begin{aligned}|\Phi(t)\rangle =& x_1\,|e_A, e_B, 0_a, 0_b\rangle + x_2\,|g_A, g_B, 1_a, 1_b\rangle + \\ & x_3\,|e_A, g_B, 0_a, 1_b\rangle + x_4\,|g_A, e_B, 1_a, 0_b\rangle + \\ & x_5\,|g_A, g_B, 0_a, 0_b\rangle\end{aligned} \tag{84}$$

One can find the coefficients in the Eq. (84) expanding the Eq. (83) as below.

$$\begin{aligned}x_1 &= \cos(\alpha)(Le^{-i\lambda^+t} + Me^{-i\lambda^-t})^2, \\ x_2 &= \cos(\alpha)(\sqrt{LM}e^{-i\lambda^+t} - \sqrt{LM}e^{-i\lambda^-t})^2, \\ x_3 &= \cos(\alpha)(Le^{-i\lambda^+t} + Me^{-i\lambda^-t})\cdot \\ &(\sqrt{LM}e^{-i\lambda^+t} - \sqrt{LM}e^{-i\lambda^-t}), \\ x_4 &= x_3, \\ x_5 &= \sin(\alpha)\end{aligned} \tag{85}$$

$$\text{where } L = \cos^2\left(\frac{\Theta}{2}\right) \quad M = \sin^2\left(\frac{\Theta}{2}\right) \tag{86}$$

1. $C_{AB}(t)$

$$\rho^{AB} = Tr_{ab}[|\Phi(t)\rangle\,\langle\Phi(t)|] \tag{87}$$

$$\begin{aligned}Tr_{0_a0_b} &= |x_1|^2\,|e_A, e_B\rangle\,\langle e_A, e_B| + |x_5|^2\,|g_A, g_B\rangle\,\langle g_A, g_B| + \\ & x1x5^*\,|e_A, e_B\rangle\,\langle g_A, g_B| + x1^*x5\,|g_A, g_B\rangle\,\langle e_A, e_B|\,, \\ Tr_{0_a,1_b} &= |x_3|^2\,|e_A, g_B\rangle\,\langle e_A, g_B|\,, \\ Tr_{1_a,0_b} &= |x_4|^2\,|g_A, e_B\rangle\,\langle g_A, e_B|\,, \\ Tr_{1_a,1_b} &= |x_2|^2\,|g_A, g_B\rangle\,\langle g_A, g_B|\end{aligned} \tag{88}$$

$$\rho^{AB} = \begin{bmatrix} |x_1|^2 & 0 & 0 & x1x5^* \\ 0 & |x_3|^2 & 0 & 0 \\ 0 & 0 & |x_4|^2 & 0 \\ x1^*x5 & 0 & 0 & |x_2|^2 + |x_5|^2 \end{bmatrix} \tag{89}$$

Since this matrix in the X form as mentioned in Eq. (68)

$$Q(t) = 2|x_1||x_5| - 2|x_3||x_4| \tag{90}$$

For the case Δ=0, tuned case $L = 1/2$ and $M = 1/2$; The eigenvalue Eq. (58) becomes:

$$\lambda^{\pm} = \omega + \frac{1}{2}G$$

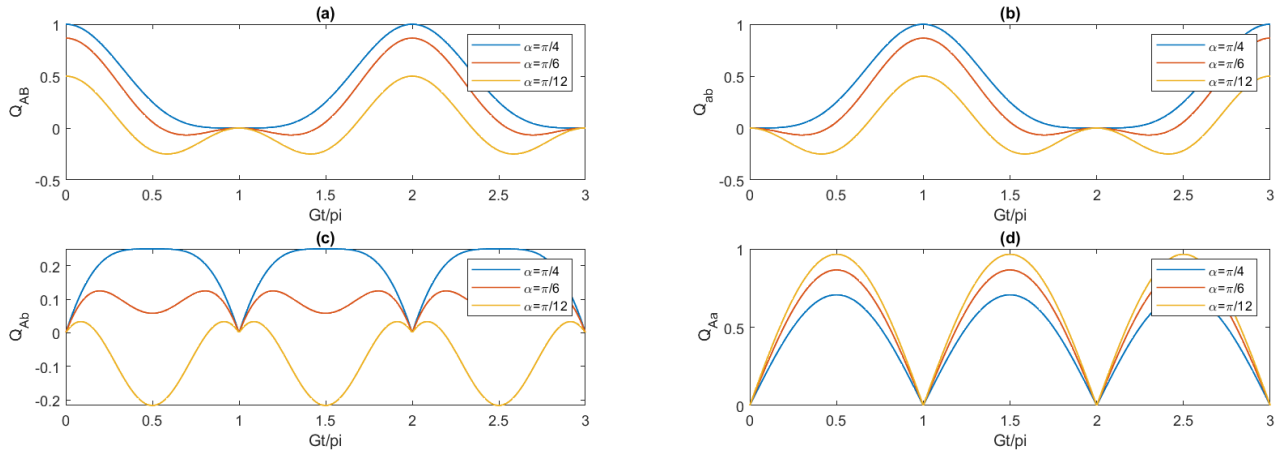

FIG. 4. Plots of Q(t) of the $|\Phi_{AB}\rangle$ initial state as a function of time and parameter α for all concurrences being C_{AB}, C_{ab}, C_{Ab}, C_{Aa} where $C_{aB} = C_{Ab}$ and $C_{Bb} = C_{Aa}$ with three different angles $\alpha = \pi/4, \alpha = \pi/6, \alpha = \pi/12$.

Calculating the absolute value of the x_1 yields:

$$\begin{aligned}
|x_1| &= |\frac{1}{2}e^{-i\lambda^+ t} + \frac{1}{2}e^{-i\lambda^- t}||\cos(\alpha)| \\
&= \frac{1}{4}|\cos(\alpha)||e^{-i\lambda^+ t} + e^{-i\lambda^- t}| \\
&= \frac{1}{4}|\cos(\alpha)||e^{-i\omega t}e^{-i\frac{Gt}{2}} + e^{-i\omega t}e^{+i\frac{Gt}{2}}| \\
&= \frac{1}{4}|\cos(\alpha)|\left|2\cos\left(\frac{Gt}{2}\right)\right|^2 \\
&= |\cos(\alpha)|\cos^2\left(\frac{Gt}{2}\right) \qquad (91)
\end{aligned}$$

Here, $e^{-i\omega t}$ becomes the global phase; thus it is omitted. Using the same procedure for the other coefficients shown in Eq. (85), $Q(t)$ is obtained as below:

$$Q(t) = \cos^2\left(\frac{Gt}{2}\right)\left[|\sin(2\alpha)| - 2\sin^2\left(\frac{Gt}{2}\right)\cos^2(\alpha)\right] \qquad (92)$$

Since the concurrence value can not take negative results, one should dismiss the negative values taking the maximum as:

$$C_{AB}(t) = max[0, Q(t)] \qquad (93)$$

Fig. 4.(a) shows the Q_{AB} for different initial angles. For the concurrence, it becomes zero when Q is negative. The entanglement non-smoothly becomes and stays zero for a finite time interval especially for the angles $\alpha \neq \pi/4$. This effect is called as "entanglement sudden death" (ESD). When the angle is $\pi/4$, the evolution is smoother and the concurrence can take the maximum value 1.

2. $C_{ab}(t)$

$$\rho^{ab} = Tr_{AB}[|\Phi(t)\rangle\langle\Phi(t)|] \qquad (94)$$

$$Q(t) = 2|x_2||x_5| - 2|x_3||x_4| \qquad (95)$$

For the tuned case:

$$Q(t) = \sin^2\left(\frac{Gt}{2}\right)\left[|\sin(2\alpha)| - 2\cos^2\left(\frac{Gt}{2}\right)\cos^2(\alpha)\right] \qquad (96)$$

Fig. 4.(b) demonstrates the Q_{ab} for different three angles. This graph can be interpolated as π/G phase lagged version of the C_{AB}. After a time interval of π/G, the state $|e_A, 0_a\rangle$ turns into to the state $|g_A, 1_a\rangle$ due to the relations shown in Eq. (76), (77). Taking into consideration of eigenvalue (58) and the time evolution of the states (76, 77) $\pi/2$ overall phase occurs. The same situation is applicable for the B and b parts. Thus it can be said that $|\Phi(t)\rangle$ is the same as $|\Phi(t + \pi/G)\rangle$. It indicates that the state observed in the perspective of atomic part at time t is the same as the state observed from the photonic part at t+π/G. Thus as mentioned, C_{ab} is the same as C_{AB} up to a phase difference of π/G.

3. $C_{Ab}(t)$

$$\rho^{Ab} = Tr_{aB}[|\Phi(t)\rangle\langle\Phi(t)|] \qquad (97)$$

$$Q(t) = 2|x_3||x_5| - 2|x_1||x_2| \qquad (98)$$

For the tuned case:

$$Q(t) = \frac{1}{2}\cos^2(\alpha)|\sin(Gt)|\,(2|\tan(\alpha)| - |\sin(Gt)|) \quad (99)$$

C_{Ab} is always less than 1; hence, the parts A and b can not be maximally entangled unlike parts A and B. (Fig. (4.c)) Moreover, for some angles, ESD occurs in a periodic manner similar to previous concurrences.

4. $C_{aB}(t)$

$$\rho^{aB} = Tr_{Ab}[|\Phi(t)\rangle\langle\Phi(t)|] \quad (100)$$

$$Q(t) = 2|x_4||x_5| - 2|x_1||x_2| \quad (101)$$

Thus, C_{Ab} is equal to C_{aB}. This can be concluded from the initial state of $|\Phi(0)\rangle$. When the transitions $A \leftrightarrow B$ and $a \leftrightarrow b$ are applied, the state remains unchanged.

5. $C_{Aa}(t)$

$$\rho^{Aa} = Tr_{Bb}[|\Phi(t)\rangle\langle\Phi(t)|] \quad (102)$$

$$Q(t) = 2|x_3||x_1 + x_2| \quad (103)$$

$$Q(t) = |\sin(Gt)|\cos^2(\alpha) \quad (104)$$

For the C_{Aa}, decreasing the angle yields higher concurrence values. (Fig. 4.(d))

6. $C_{Bb}(t)$

From the initial state symmetry which was previously mentioned in C_{aB}, one can directly say that $C_{Bb}(t) = C_{Aa}(t)$

B. Partially Entangled State $|\Psi_{AB}\rangle$

$$|\Psi(0)\rangle = |\Psi_{AB}\rangle \otimes |0_a, 0_b\rangle \quad (105)$$

$$|\Psi(0)\rangle = (\cos(\alpha)\,|e_A, g_B\rangle + \sin(\alpha)\,|g_A, e_B\rangle) \otimes |0_a, 0_b\rangle \quad (106)$$

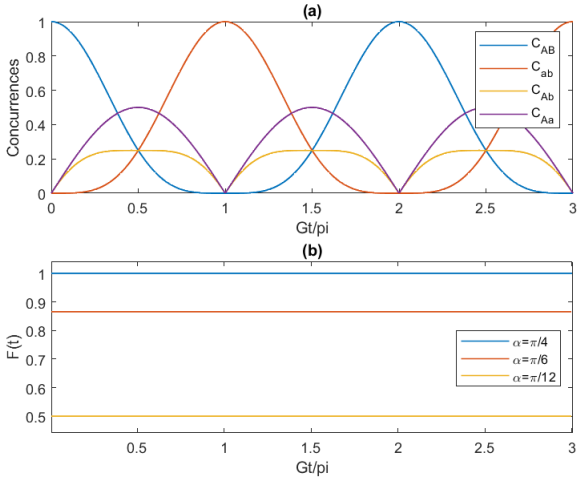

FIG. 5. (a) Plot for the all concurrences of $|\Phi_{AB}\rangle$ initial state as a function of time where $\alpha = \pi/4$. (b) Conservation of the entanglement of $|\Phi_{AB}\rangle$ initial state for different angles α

Following the same procedure used in the $|\Phi_{AB}\rangle$, the initial state can be written in terms of the dressed states given in Equations (73), (74), (75):

$$\begin{aligned}|\Psi(0)\rangle =& \cos(\alpha)(c\,|\Psi_1^+\rangle_A - s\,|\Psi_1^-\rangle_A) \otimes |\Psi_0\rangle_B + \\ & \sin(\alpha)\,|\Psi_0\rangle_A \otimes (c\,|\Psi_1^+\rangle_B - s\,|\Psi_1^-\rangle_B)\end{aligned} \quad (107)$$

Using the Equation (81), $|\Psi(t)\rangle$ can be written as:

$$\begin{aligned}|\Psi(t)\rangle =& \cos(\alpha)(ce^{-i\lambda^+ t}\,|\Psi_1^+\rangle_A - se^{-i\lambda^- t}\,|\Psi_1^-\rangle_A) \otimes |\Psi_0\rangle_B + \\ & \sin(\alpha)\,|\Psi_0\rangle_A \otimes (ce^{-i\lambda^+ t}\,|\Psi_1^+\rangle_B - se^{-i\lambda^- t}\,|\Psi_1^-\rangle_B)\end{aligned} \quad (108)$$

Reverting back to the bare basis using the dressed states 73, 74, 75:

$$\begin{aligned}|\Psi(t)\rangle =& \cos(\alpha)\Big[(ce^{-i\lambda^+ t} + se^{-i\lambda^- t})\,|e_A, 0_a\rangle + \\ & (se^{-i\lambda^+ t} - ce^{-i\lambda^- t})\,|g_A, 1_a\rangle\Big] \otimes |g_B, 0_B\rangle + \\ & \sin(\alpha)\,|g_A, 0_a\rangle \otimes \Big[(ce^{-i\lambda^+ t} + se^{-i\lambda^- t})\,|e_B, 0_b\rangle + \\ & (se^{-i\lambda^+ t} - ce^{i\lambda^- t})\,|g_B, 1_b\rangle\Big]\end{aligned} \quad (109)$$

Let's write this equation as below

$$\begin{aligned}|\Psi(t)\rangle =& x_1\,|e_A, g_B, 0_a, 0_b\rangle + x_2\,|g_A, e_B, 0_a, 0_b\rangle + \\ & x_3\,|g_A, g_B, 1_a, 0_b\rangle + x_4\,|g_A, g_B, 0_a, 1_b\rangle\end{aligned} \quad (110)$$

where

$$\begin{aligned} x_1 &= \cos(\alpha)(Le^{-i\lambda^+ t} + Me^{-i\lambda^- t}) \\ x_2 &= \sin(\alpha)(Le^{-i\lambda^+ t} + Me^{-i\lambda^- t}) \\ x_3 &= \cos(\alpha)(\sqrt{LM}e^{-i\lambda^+ t} - \sqrt{LM}e^{-i\lambda^- t}) \\ x_4 &= \sin(\alpha)(\sqrt{LM}e^{-i\lambda^+ t} - \sqrt{LM}e^{-i\lambda^- t}) \end{aligned} \tag{111}$$

L and M are the same with Eq. (86)

1. $C_{AB}(t)$

$$\rho^{AB} = Tr_{ab}[|\Psi(t)\rangle \langle\Psi(t)|] \tag{112}$$

$$\begin{aligned} &Tr_{0_a 0_b} = |x_1|^2 |e_A, g_B\rangle \langle e_A, g_B| + |x_2|^2 |g_A, e_B\rangle \langle g_A, e_B| + \\ &x1x2^* |e_A, g_B\rangle \langle g_A, e_B| + x1^* x2 |g_A, e_B\rangle \langle e_A, g_B| \\ &Tr_{0_a, 1_b} = |x_4|^2 |g_A, g_B\rangle \langle g_A, g_B|, \\ &Tr_{1_a, 0_b} = |x_3|^2 |g_A, g_B\rangle \langle g_A, g_B|, \\ &Tr_{1_a, 1_b} = 0 \end{aligned} \tag{113}$$

$$\rho^{AB} = \begin{bmatrix} |x_3|^2 + |x_4|^2 & 0 & 0 & 0 \\ 0 & |x_2|^2 & x1x2^* & 0 \\ 0 & x1^* x2 & |x_1|^2 & 0 \\ 0 & 0 & 0 & 0 \end{bmatrix} \tag{114}$$

Since this matrix in the X form as mentioned in the Section 2

$$Q(t) = 2|x_1||x_2| \tag{115}$$

For the case Δ=0, tuned case $L = 1/2$ and $M = 1/2$; therefore, $Q(t)$ becomes:

$$Q(t) = |\sin(2\alpha)| \cos^2\left(\frac{Gt}{2}\right) \tag{116}$$

2. $C_{ab}(t)$

$$\rho^{ab} = Tr_{AB}[|\Psi(t)\rangle \langle\Psi(t)|] \tag{117}$$

$$Q(t) = 2|x_3||x_3| \tag{118}$$

For the tuned case:

$$Q(t) = |\sin(2\alpha)| \sin^2\left(\frac{Gt}{2}\right) \tag{119}$$

Similar to C_{ab} of $|\Phi_A\rangle$, one can say that C_{ab} is the same as C_{AB} up to a phase difference of π/G. (Fig. (6.(a)-(b))

3. $C_{Ab}(t)$

$$\rho^{Ab} = Tr_{aB}[|\Psi(t)\rangle \langle\Psi(t)|] \tag{120}$$

$$Q(t) = 2|x_1||x_4| \tag{121}$$

For the tuned case:

$$Q(t) = \frac{1}{2}|\sin(2\alpha)||\sin(Gt)| \tag{122}$$

4. $C_{aB}(t)$

Under the transformation $A \leftrightarrow B$, $a \leftrightarrow b$ and $\cos(\alpha) \leftrightarrow \sin(\alpha)$ the state remains unchanged. Therefore, this transformation does not change the concurrence equation yielding $C_{Ab} = C_{aB}$.

5. $C_{Aa}(t)$

$$\rho^{Aa} = Tr_{Bb}[|\Psi(t)\rangle \langle\Psi(t)|] \tag{123}$$

$$Q(t) = 2|x_1||x_3| \tag{124}$$

$$Q(t) = |\sin(Gt)| \cos^2(\alpha) \tag{125}$$

6. $C_{Bb}(t)$

Under the transformation $A \leftrightarrow B$, $a \leftrightarrow b$ and $\cos(\alpha) \leftrightarrow \sin(\alpha)$ the state remains unchanged. Here the concurrence equation will change according to transformation:

$$Q(t) = \sin^2(\alpha)|\sin(Gt)| \tag{126}$$

To sum up, in this section the entanglement dynamics of several subsystems in a four-qubit model in which two atoms are locally coupled to the modes of their cavities is examined. In this model, there are no interactions between the two cavities as shown in Fig. (2). The evolution of the entanglement is a pure information-exchange evolution, meaning there is no decoherence process, differs from Section (II). Two sets of pure initial states are investigated being partially entangled $|\Phi_{AB}\rangle$ and $|\Psi_{AB}\rangle$. For the $|\Phi_{AB}\rangle$ initial state two photons may be present simultaneously (Eq. 84); whereas for $|\Psi_{AB}\rangle$ initial case more than one photon never exist (Eq. 110). For all concurrences, the cavity and the atom are assumed to be in resonance. Entanglement sudden death (ESD) occurs for the $|\Phi_{AB}\rangle$ initial state, and concurrence remains zero

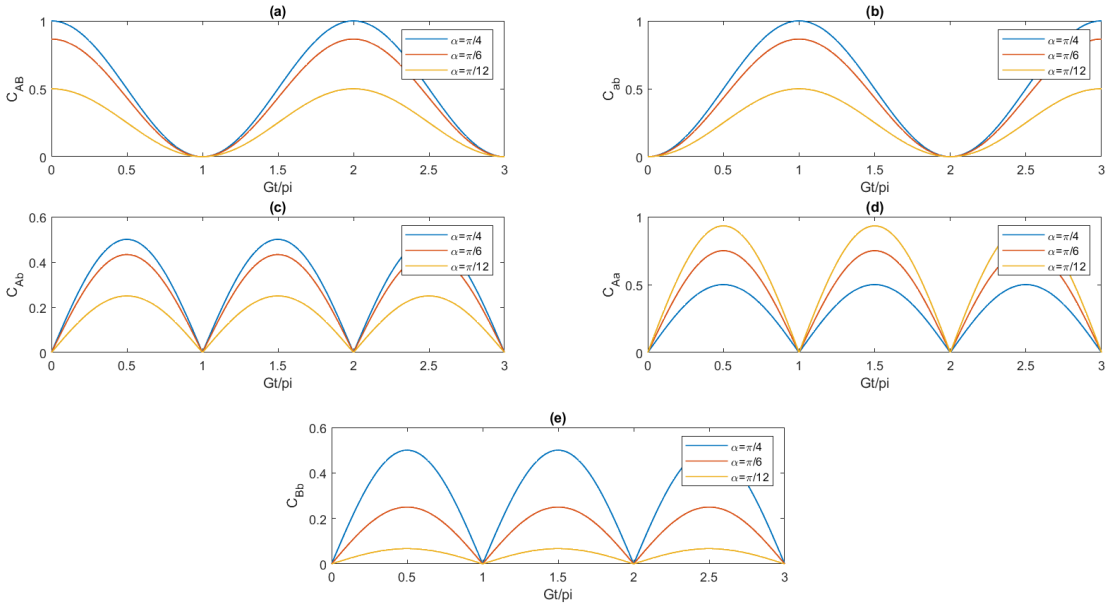

FIG. 6. Plots of concurrences of the $|\Psi_{AB}\rangle$ initial state as a function of time and parameter α for all concurrences being C_{AB}, C_{ab}, C_{Ab}, C_{Aa}, C_{Bb} where $C_{aB} = C_{Ab}$.

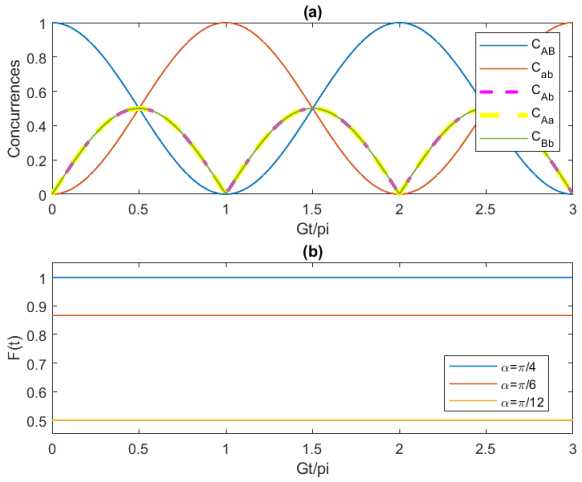

FIG. 7. (a) Plot for the all concurrences of $|\Psi_{AB}\rangle$ initial state as a function of time where $\alpha = \pi/4$. (b) Conservation of the entanglement of $|\Psi_{AB}\rangle$ initial state for different angles α

for finite time intervals which can be seen in Fig. (4). In this figure, $Q(t)$ is plotted; the concurrence is taken as 0 for the negative values of $Q(t)$ given in Eq. (93). It can be seen that decreasing α yields smaller concurrences except for C_{Aa} and C_{Bb}. Moreover, due to the non-existence of decoherence, the entanglement can rebirth. For the $|\Psi_{AB}\rangle$ initial state, there is no ESD occurring (Fig. (6)). The existence of the additional term in Eq. 84 leads to negative terms in the Q function yielding ESD. These negative terms in $|\Phi_{AB}(t)\rangle$ cause entanglement leak. Overall, if the atom-atom subsystem is initially constructed in an entangled state, the local atom-cavity couplings provide non-local entanglement between the cavities in addition to local entanglement between an atom and its cavity. Entanglement transfer from atomic to photonic variables can be seen as the cause of the cavity-pair's entanglement gain. For the ideal JC model, it can be observed that the entanglement is conserved. Entanglement conservation for $|\Phi_{AB}\rangle$:

$$Q_{AB} + Q_{ab} + 2|\tan(\alpha)|Q_{Aa} - 2Q_{Ab} = |\sin(2\alpha)| \quad (127)$$

Entanglement conservation for $|\Psi_{AB}\rangle$:

$$(Q_{AB} + Q_{ab}) + (Q_{Ab} - Q_{aB}) + (\sin^2(\alpha)Q_{Aa} - \cos^2(\alpha)Q_{Bb}) = |\sin(2\alpha)| \quad (128)$$

In [2], the same conservation equation (127) is used for both $|\Phi_{AB}\rangle$ and $|\Psi_{AB}\rangle$. Even though, the same results occur, here different conservation relation is employed (128). Since the concurrences for C_{Aa} and C_{Bb} are not the same for $|\Psi_{AB}\rangle$ unlike $|\Phi_{AB}\rangle$. In the Figs. (5.b) and (7.b), conserved entanglements are demonstrated for the different α values. The creation of entanglement and a system's temporal memory are related. The memory effect in the JC model results from the photons absorbed by the cavity modes being coupled back to the atom in a limited amount of time.

IV. MORE PHOTONS CASE

In this section, we have the same system shown in Fig. (2). The Hamiltonian and the eigenstates of the JC Model are same as Eqs. (64) to (60, 61). Moreover, the same initial atom states are studied here which are shown in Eqs. (66) and (67). Difference between the Section III is the possible photon number in the cavity. In Section III, there can be at maximum one photon in the cavity. However, in this case, we can have more than one photon inside the cavity.

A. Partially Entangled Bell State $|\Phi_{AB}\rangle$

$$|\Phi(0)\rangle = |\Phi_{AB}\rangle \otimes |n_a - 1, n_b - 1\rangle \tag{129}$$

$$|\Phi(0)\rangle = (\cos(\alpha)\,|e_A, e_B\rangle + \sin(\alpha)\,|g_A, g_B\rangle) \otimes |n_a - 1, n_b - 1\rangle \tag{130}$$

Here, n is taken from 1; thus, n-1 notation is used. One can write the initial state of the system in terms of the dressed states. For the more photon case, bare states can be stated in terms of the dressed states become:

$$|g, n_a - 1\rangle = |\Psi_{n_a-1}\rangle \tag{131}$$
$$|e_A, n_a - 1\rangle = c\,|\Psi^+_{n_a}\rangle - s\,|\Psi^-_{n_a}\rangle \tag{132}$$
$$|g_A, n_a\rangle = s\,|\Psi^+_{n_a}\rangle + c\,|\Psi^-_{n_a}\rangle \tag{133}$$

Here c and s are shown in Eq. (241).

$$\begin{aligned}|\Phi(0)\rangle =& \cos(\alpha)\,|e_A, n_a - 1\rangle \otimes |e_B, n_b - 1\rangle + \\ & \sin(\alpha)\,|g_A, n_a - 1\rangle \otimes |g_B, n_b - 1\rangle\end{aligned} \tag{134}$$

$$\begin{aligned}|\Phi(0)\rangle =& \cos(\alpha)(c\,|\Psi^+_{n_a}\rangle_A - s\,|\Psi^-_{n_a}\rangle_A) \otimes (c\,|\Psi^+_{n_b}\rangle_B - s\,|\Psi^-_{n_b}\rangle_B) + \\ & \sin(\alpha)\,|\Psi_{n_a-1}\rangle \otimes |\Psi_{n_b-1}\rangle\end{aligned} \tag{135}$$

Using Eq.(81) time evolution of the $|\Phi\rangle$:

$$\begin{aligned}|\Phi(t)\rangle =& \cos(\alpha)(ce^{-i\lambda^+ t}\,|\Psi^+_{n_a}\rangle_A - se^{-i\lambda^- t}\,|\Psi^-_{n_a}\rangle_A) \otimes \\ & (ce^{-i\lambda^+ t}\,|\Psi^+_{n_b}\rangle_B - se^{-i\lambda^- t}\,|\Psi^-_{n_b}\rangle_B) + \\ & \sin(\alpha)\,|\Psi_{n_a-1}\rangle_A \otimes |\Psi_{n_a-1}\rangle_B\end{aligned} \tag{136}$$

To take partial trace over individual atoms or cavities, one needs to revert to the bare bases. Writing down the Eq. (136) in terms of the bare basis:

$$\begin{aligned}|\Phi(t)\rangle =& \cos(\alpha)\left[(c^2e^{-i\lambda^+ t} + s^2e^{-i\lambda^- t})\,|e_A, n_a - 1\rangle + \right. \\ & \left.(cse^{-i\lambda^+ t} - cse^{-i\lambda^- t})\,|g_A, n_a\rangle\right] \otimes \\ & \cos(\alpha)\left[(c^2e^{-i\lambda^+ t} + s^2e^{-i\lambda^- t})\,|e_B, n_b - 1\rangle + \right. \\ & \left.(cse^{-i\lambda^+ t} - cse^{i\lambda^- t})\,|g_B, n_b\rangle\right] + \\ & \sin(\alpha)\,|g_A, n_a - 1\rangle \otimes |g_B, n_b - 1\rangle\end{aligned} \tag{137}$$

Let's write this equation as below

$$\begin{aligned}|\Phi(t)\rangle =& x_1\,|e_A, e_B, n_a - 1, n_b - 1\rangle + x_2\,|g_A, g_B, n_a, n_b\rangle + \\ & x_3\,|e_A, g_B, n_a - 1, n_b\rangle + x_4\,|g_A, e_B, n_a, n_b - 1\rangle + \\ & x_5\,|g_A, g_B, n_a - 1, n_b - 1\rangle\end{aligned} \tag{138}$$

One can find the coefficients in the Eq. (138) expanding the Eq. (137). Coefficients can be found the same as in Eq. (85). One can easily deduce that each concurrence equation will be the same as in Section III. The only difference arises from the G_n factor which is proportional to the photon number.

1. $C_{AB}(t)$

$$Q(t) = \cos^2\left(\frac{G_n t}{2}\right)\left[|\sin(2\alpha)| - 2\sin^2\left(\frac{G_n t}{2}\right)\cos^2(\alpha)\right] \tag{139}$$

2. $C_{ab}(t)$

$$Q(t) = \sin^2\left(\frac{G_n t}{2}\right)\left[|\sin(2\alpha)| - 2\cos^2\left(\frac{G_n t}{2}\right)\cos^2(\alpha)\right] \tag{140}$$

3. $C_{Ab}(t)$

$$Q(t) = \frac{1}{2}\cos^2(\alpha)|\sin(G_n t)|\,(2|\tan(\alpha)| - |\sin(G_n t)|) \tag{141}$$

4. $C_{aB}(t)$

C_{Ab} is equal to C_{aB}. This can be concluded from the initial state of $|\Phi(0)\rangle$. When the transitions $A \leftrightarrow B$ and $a \leftrightarrow b$ are applied, the state remains unchanged.

5. $C_{Aa}(t)$

$$Q(t) = |\sin(G_n t)| \cos^2(\alpha) \tag{142}$$

6. $C_{Bb}(t)$

From the initial state symmetry which was previously mentioned in C_{aB}, one can directly say that $C_{Bb}(t) = C_{Aa}(t)$

B. Partially Entangled Bell State $|\Psi_{AB}\rangle$

$$|\Psi(0)\rangle = |\Psi_{AB}\rangle \otimes |n_a - 1, n_b - 1\rangle \tag{143}$$

$$|\Psi(0)\rangle = (\cos(\alpha)\,|e_A, g_B\rangle + \sin(\alpha)\,|g_A, e_B\rangle) \otimes |n_a - 1, n_b - 1\rangle \tag{144}$$

Following the same procedure used in the $|\Phi_{AB}\rangle$, the initial state can be written in terms of the dressed states given in Equations (131), (132), (133):

$$\begin{aligned}|\Psi(0)\rangle = &\cos(\alpha)(c\,|\Psi^+_{n_a}\rangle_A - s\,|\Psi^-_{n_a}\rangle_A) \otimes |\Psi_{n_b-1}\rangle_B + \\ &\sin(\alpha)\,|\Psi_{n_a-1}\rangle_A \otimes (c\,|\Psi^+_{n_b}\rangle_B - s\,|\Psi^-_{n_b}\rangle_B)\end{aligned} \tag{145}$$

Using the Equation (81), $|\Psi(t)\rangle$ can be written as:

$$\begin{aligned}|\Psi(t)\rangle = &\cos(\alpha)(ce^{-i\lambda^+ t}\,|\Psi^+_1\rangle_A - se^{-i\lambda^- t}\,|\Psi^-_1\rangle_A) \otimes |\Psi_0\rangle_B + \\ &\sin(\alpha)\,|\Psi_0\rangle_A \otimes (ce^{-i\lambda^+ t}\,|\Psi^+_1\rangle_B - se^{-i\lambda^- t}\,|\Psi^-_1\rangle_B)\end{aligned} \tag{146}$$

Reverting back to the bare basis using the dressed states 131, 132, 133:

$$\begin{aligned}|\Psi(t)\rangle = &\cos(\alpha)\Big[(ce^{-i\lambda^+ t} + se^{-i\lambda^- t})\,|e_A, n_a - 1\rangle + \\ &(se^{-i\lambda^+ t} - ce^{-i\lambda^- t})\,|g_A, n_a\rangle\Big] \otimes |g_B, n_B - 1\rangle + \\ &\sin(\alpha)\,|g_A, n_a - 1\rangle \otimes \Big[(ce^{-i\lambda^+ t} + se^{-i\lambda^- t}) \\ &|e_B, n_b - 1\rangle + (se^{-i\lambda^+ t} - ce^{i\lambda^- t})\,|g_B, n_b\rangle\Big]\end{aligned} \tag{147}$$

Let's write this equation as below

$$\begin{aligned}|\Psi(t)\rangle = &x_1\,|e_A, g_B, n_a - 1, n_b - 1\rangle + \\ &x_2\,|g_A, e_B, n_a - 1, n_b - 1\rangle + \\ &x_3\,|g_A, g_B, n_a, n_b - 1\rangle + x_4\,|g_A, g_B, n_a - 1, n_b\rangle\end{aligned} \tag{148}$$

One can find the coefficients in the Eq. (148) expanding the Eq. (147). Coefficients can be found the same as in Eq. (111). One can easily deduce that each concurrence equation will be the same as in Section III. The only difference arises from the G_n factor which is proportional to the photon number.

1. $C_{AB}(t)$

$$Q(t) = |\sin(2\alpha)| \cos^2\left(\frac{G_n t}{2}\right) \tag{149}$$

2. $C_{ab}(t)$

$$Q(t) = |\sin(2\alpha)| \sin^2\left(\frac{G_n t}{2}\right) \tag{150}$$

3. $C_{Ab}(t)$

$$Q(t) = \frac{1}{2}|\sin(2\alpha)||\sin(G_n t)| \tag{151}$$

4. $C_{aB}(t)$

Under the transformation $A \leftrightarrow B$, $a \leftrightarrow b$ and $\cos(\alpha) \leftrightarrow \sin(\alpha)$ the state remains unchanged. Therefore, this transformation does not change the concurrence equation yielding $C_{Ab} = C_{aB}$.

5. $C_{Aa}(t)$

$$Q(t) = |\sin(G_n t)| \cos^2(\alpha) \tag{152}$$

6. $C_{Bb}(t)$

From the initial state symmetry which was previously mentioned in C_{aB}, one can directly say that $C_{Bb}(t) = C_{Aa}(t)$

As highlighted previously, the only difference with the one-photon cavity case (Section III) arises from the G_n, n photon Rabi frequency. From Fig. 8.(a), the increased frequency of the C_{AB} of the $|\Phi_{AB}\rangle$ with increasing photon number can be seen. Since the frequency increases the finite time of the disentanglement decreases as well. Moreover, since the G_n factor is proportional to the

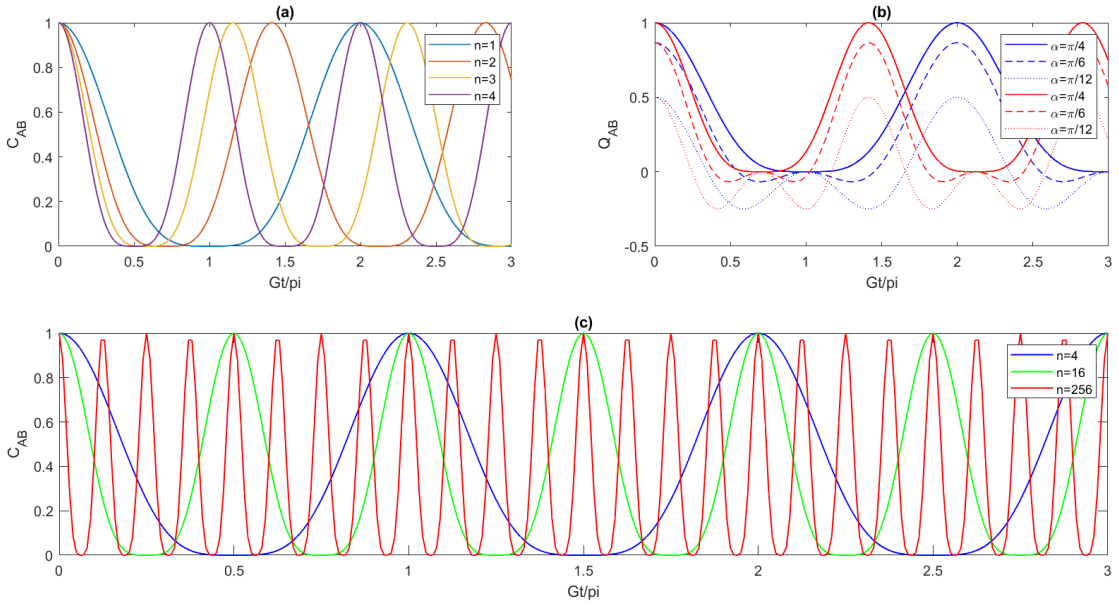

FIG. 8. (a) Plot of C_{AB} of Φ_{AB} initial state at fixed $\alpha = \pi/4$ as a fınction of time for different photon numbers inside the cavity. (b) Plot of Q_{AB} for different angles in which blue and red lines resemble n=1 and n=16 respectively. (c) Plot of C_{AB} for different numbers of photons at $\alpha = \pi/4$

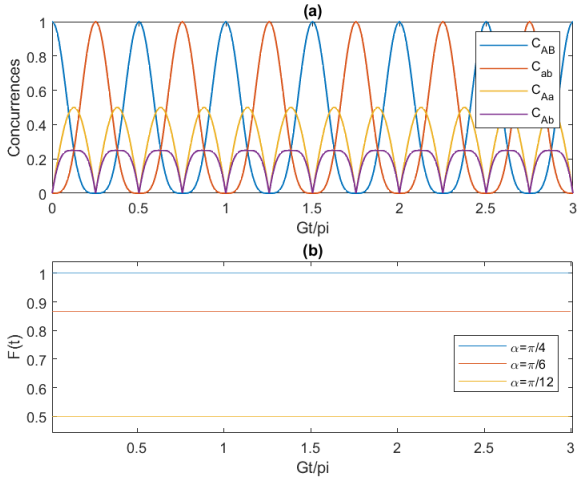

FIG. 9. (a) Plot for the all concurrences of $|\Phi_{AB}\rangle$ initial state as a function of time where $\alpha = \pi/4$ and n=16. (b) Conservation of the entanglement of $|\Phi_{AB}\rangle$ initial state for different angles α

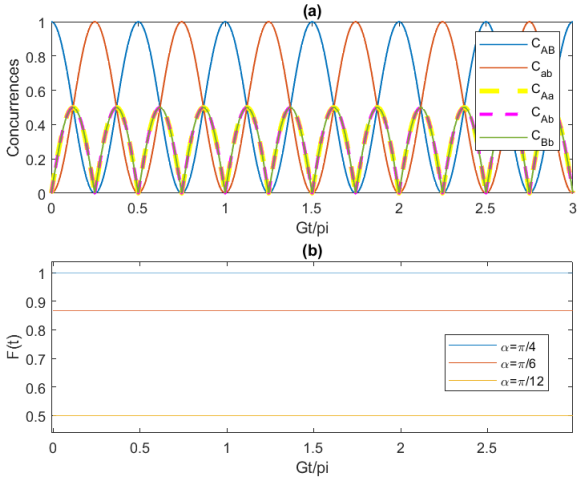

FIG. 10. (a) Plot for the all concurrences of $|\Psi_{AB}\rangle$ initial state as a function of time where $\alpha = \pi/4$ and n=16. (b) Conservation of the entanglement of $|\Psi_{AB}\rangle$ initial state for different angles α

square root of the number of photons inside the cavity one can deduct that the periods of the concurrences become proportional to the n. For instance, in Fig. 8.(c), initially the number of photons is taken as 4, for n=16, and n=256 the frequency increased by 2 and 16 times respectively. Changing the angle of the initial state gives similar results to the previous sections. One can expect that the other concurrences show similar changes like period decrease proportional to the square root of the number of photons. (Figs. (9.a)-(10.a)). Likewise in the previous section, the entanglement conservation can be observed provided with the same equations. (127,128). The conserved entanglement can be seen from the Figs. 9.(b) and 10.(b). The results are same as the conservation examined in the previous section.

V. COHERENT STATE CASE

This section examines another different initial state condition which is the coherent state in the same system shown in Fig. (2). A coherent state is a specific quantum state of a quantum harmonic oscillator, frequently described as a state with dynamics most similar to that of a classical harmonic oscillator. Coherent states are also known for their minimum possible uncertainty in the position and momentum measurements, which means they have the smallest uncertainty allowed by the Heisenberg uncertainty principle. They have a stable phase relationship between position and momentum components. The coherent states are expressed as eigenvectors of the lowering operator:

$$\hat{a}\left|\alpha\right\rangle = \alpha\left|\alpha\right\rangle \quad \alpha \in \mathbb{C} \tag{153}$$

$$\alpha = |\alpha| e^{i\theta} \tag{154}$$

where $|a|$ and θ are the amplitude and the phase of the coherent state. The lowering operator affects the Fock state:

$$\hat{a}\left|n\right\rangle = \sqrt{n}\left|n-1\right\rangle \tag{155}$$

The coherent state can be described as infinite sum of the Fock states:

$$\left|\alpha\right\rangle = e^{-|\alpha|^2/2}\sum_{n=0}^{\infty}\frac{\alpha^n}{\sqrt{n!}}\left|n\right\rangle \tag{156}$$

The displacement operator is a mathematical operator used in quantum mechanics to describe the displacement of a quantum state in phase space. This operator acts on a quantum state, such as a coherent state, and shifts it in both position and momentum space. Specifically, for a quantum harmonic oscillator, the displacement operator is defined as:

$$\hat{D} = e^{\alpha\hat{a}^+}e^{-\alpha\hat{a}}e^{-\frac{|\alpha|^2}{2}} \tag{157}$$

$$\left|\alpha\right\rangle = \hat{D}(\alpha)\left|0\right\rangle \tag{158}$$

In this system, initially, the cavity a and b are in the coherent states $\left|\alpha_A\right\rangle$ and $\left|\alpha_B\right\rangle$ respectively. Moreover, the same initial atom states are studied here which are shown in Eqs. (66) and (67).

A. Partially Entangled Bell State $\left|\Phi_{AB}\right\rangle$

$$\left|\Phi(0)\right\rangle = \left|\Phi_{AB}\right\rangle \otimes \left|\alpha_A, \alpha_B\right\rangle \tag{159}$$

$$\left|\Phi(0)\right\rangle = (\cos(\theta)\left|e_A, e_B\right\rangle + \sin(\theta)\left|g_A, g_B\right\rangle) \otimes \left|\alpha_A, \alpha_B\right\rangle \tag{160}$$

$$\left|e_A, \alpha_A\right\rangle = \left|e_A, \hat{D}(\alpha_A)\left|0\right\rangle\right\rangle = \hat{D}(\alpha_A)\left|e_A, 0_a\right\rangle \tag{161}$$

where the coherent state $\left|\alpha_A\right\rangle$ is represented with the displacement operator. This process can be also applied to the coherent state in the cavity b:

$$\begin{aligned}\left|\Phi(0)\right\rangle =& \cos(\theta)\left(\hat{D}(\alpha_A)\left|e_A, 0_a\right\rangle \otimes \hat{D}(\alpha_B)\left|e_B, 0_b\right\rangle\right) + \\ & \sin(\theta)\left(\hat{D}(\alpha_A)\left|g_A, 0_a\right\rangle \otimes \hat{D}(\alpha_B)\left|g_B, 0_b\right\rangle\right)\end{aligned} \tag{162}$$

As can be seen from Eq. (162), the initial state of the system $\left|\Phi\right\rangle$ becomes similar to the initial state for the one-photon cavity case (72). Here, one should notice that the angle α is changed to θ to prevent the possible confusion between the coherent state $\left|\alpha\right\rangle$ and Bell state angle α. Expanding the Eq. (162) in terms of the dressed states (76), (77):

$$\begin{aligned}\left|\Phi(0)\right\rangle =& \cos(\theta)[\hat{D}(\alpha_A)(c\left|\Psi_1^+\right\rangle_A - s\left|\Psi_1^-\right\rangle_A)\otimes \\ & \hat{D}(\alpha_B)(c\left|\Psi_1^+\right\rangle_B - s\left|\Psi_1^-\right\rangle_B)]+ \\ & \sin(\theta)\hat{D}(\alpha_A)\left|\Psi_0\right\rangle_A \otimes \hat{D}(\alpha_B)\left|\Psi_0\right\rangle_B\end{aligned} \tag{163}$$

Then, time evolution of the system can be found using the Schrodinger relation (81):

$$\begin{aligned}\left|\Phi(t)\right\rangle =& \cos(\theta)[\hat{D}(\alpha_A)(ce^{-i\lambda^+ t}\left|\Psi_1^+\right\rangle_A - se^{-i\lambda^- t}\left|\Psi_1^-\right\rangle_A)\otimes \\ & \hat{D}(\alpha_B)(ce^{-i\lambda^+ t}\left|\Psi_1^+\right\rangle_B - se^{-i\lambda^- t}\left|\Psi_1^-\right\rangle_B)]+ \\ & \sin(\theta)[\hat{D}(\alpha_A)\left|\Psi_0\right\rangle_A \otimes \hat{D}(\alpha_B)\left|\Psi_0\right\rangle_B]\end{aligned} \tag{164}$$

Reverting back to the bare basis states consisting of e and g:

$$\begin{aligned}\left|\Phi(t)\right\rangle =& \cos(\theta)[\hat{D}(\alpha_A)(ce^{-i\lambda^+ t}(c\left|e_A, 0_a\right\rangle + s\left|g_A, 1_a\right\rangle)- \\ & se^{-i\lambda^- t}(-s\left|e_A, 0_a\right\rangle + c\left|g_A, 1_a\right\rangle)\otimes \\ & \hat{D}(\alpha_B)(ce^{-i\lambda^+ t}(c\left|e_B, 0_b\right\rangle + s\left|g_B, 1_b\right\rangle)- \\ & se^{-i\lambda^- t}(-s\left|e_B, 0_b\right\rangle + c\left|g_B, 1_b\right\rangle)]+ \\ & \sin(\theta)\hat{D}(\alpha_A)\left|g_A, 0_a\right\rangle \otimes \hat{D}(\alpha_B)\left|g_B, 0_b\right\rangle\end{aligned} \tag{165}$$

Thus final version of the time evolved system equation can be written as in the form of:

$$\begin{aligned}\left|\Phi(t)\right\rangle =& x_1'\left|e_A, e_B, 0_a, 0_b\right\rangle + x_2'\left|g_A, g_B, 1_a, 1_b\right\rangle + \\ & x_3'\left|e_A, g_B, 0_a, 1_b\right\rangle + x_4'\left|g_A, e_B, 1_a, 0_b\right\rangle + \\ & x_5'\left|g_A, g_B, 0_a, 0_b\right\rangle\end{aligned} \tag{166}$$

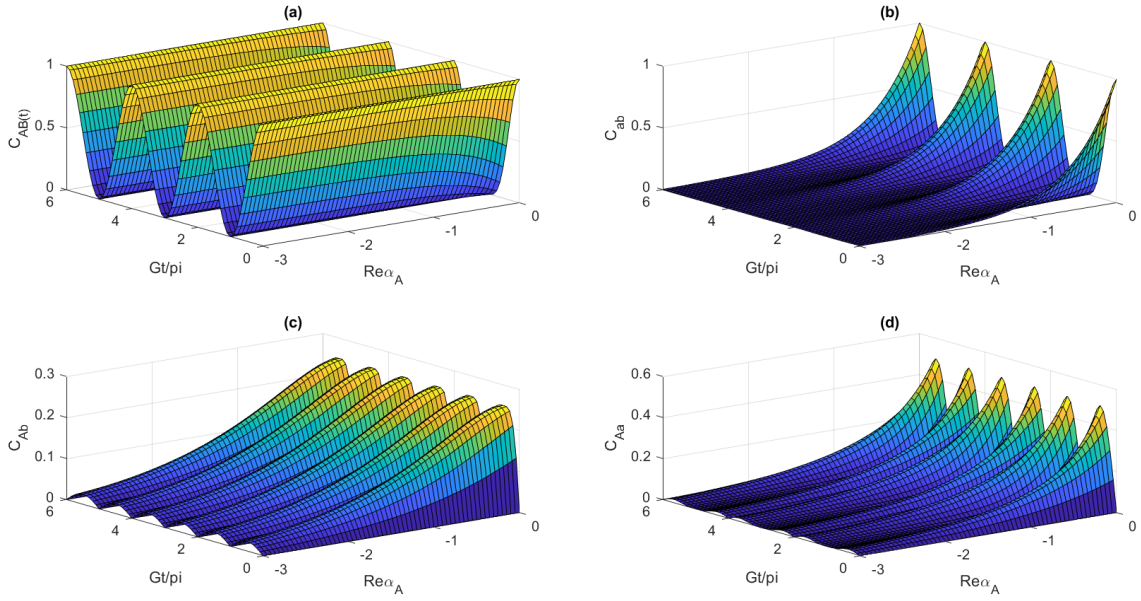

FIG. 11. (a) Plot for C_{AB} of $|\Phi\rangle$ as a function of time and $\Re(\alpha_A)$ where $\theta = \pi/4$. (b) Plot for C_{ab} as a function of time and $\Re(\alpha_A)$ where $\theta = \pi/4$. (c) Plot for C_{Ab} as a function of time and $\Re(\alpha_A)$ where $\theta = \pi/4$. (d) Plot for C_{Aa} as a function of time and $\Re(\alpha_A)$ where $\theta = \pi/4$. Similar to other Φ_{AB} initial state cases, C_{aB}, C_{Bb} are not shown since $C_{aB} = C_{Ab}$ and $C_{Bb} = C_{Aa}$.

where the coefficients are:

$$\begin{aligned} x_1' &= \hat{D}(\alpha_A) \otimes \hat{D}(\alpha_B) x_1 \\ x_2' &= \hat{D}(\alpha_A) \otimes \hat{D}(\alpha_B) x_2 \\ x_3' &= \hat{D}(\alpha_A) \otimes \hat{D}(\alpha_B) x_3 \\ x_4' &= x_3' \\ x_5' &= \hat{D}(\alpha_A) \otimes \hat{D}(\alpha_B) x_5 \end{aligned} \tag{167}$$

In the Eq. (167), x_1, x_2, x_3, x_4 are the same coefficients in the Eq. (85). Since 1 photon could exist in Eq. (166), one needs to find the effect of the displacement operator on the $|1_a\rangle$ and $|1_b\rangle$. Previously, the effect on $|0_a\rangle$ is shown in Eq. (161). The process can be shown in terms of $\hat{D}(\alpha_A + 1)$ as below:

$$\hat{D}(\alpha_A)|1\rangle = \hat{D}(\alpha_A)\hat{D}(1)|0\rangle = X\hat{D}(\alpha_A + 1) \tag{168}$$

X term can be found using the below manipulation sequences:

$$\begin{aligned} \hat{D}(\alpha_A) &= e^{\alpha_A \hat{a}^\dagger} e^{-\alpha_A^* \hat{a}} e^{-\frac{|\alpha_A|^2}{2}} \\ \hat{D}(1) &= e^{1.\hat{a}^\dagger} e^{-1.\hat{a}} e^{-\frac{1}{2}} \\ \hat{D}(\alpha_A)\hat{D}(1) &= e^{(\alpha_A+1)\hat{a}^\dagger} e^{-(\alpha_A^*+1)\hat{a}} e^{-\frac{|\alpha_A|^2}{2}} e^{-\frac{1}{2}} \\ \hat{D}(\alpha_A + 1) &= e^{(\alpha_A+1)\hat{a}^\dagger} e^{-(\alpha_A^*+1)\hat{a}} e^{-\frac{|\alpha_A+1|^2}{2}} \\ e^{-\frac{|\alpha_A|^2}{2}} e^{-\frac{1}{2}} &= X e^{-\frac{|\alpha_A+1|^2}{2}} \\ e^{-\frac{|\alpha_A|^2}{2}} e^{-\frac{1}{2}} &= X e^{-\frac{(\alpha_A+1)(\alpha_A^*+1)}{2}} \\ e^{-\frac{|\alpha_A|^2}{2}} e^{-\frac{1}{2}} &= X e^{-\frac{|\alpha_A|^2}{2}} e^{-\frac{\alpha_A}{2}} e^{-\frac{\alpha_A^*}{2}} e^{-\frac{1}{2}} \\ X &= e^{\frac{\alpha_A}{2}} e^{\frac{\alpha_A^*}{2}} = e^{\Re(\alpha_A)} \end{aligned} \tag{169}$$

Thus, Eq. (166) becomes:

$$\begin{aligned} |\Phi(t)\rangle =& x_1 |e_A, e_B, \alpha_A, \alpha_B\rangle + \\ & x_2 e^{\Re(\alpha_A)+\Re(\alpha_B)} |g_A, g_B, \alpha_A + 1, \alpha_B + 1\rangle + \\ & x_3 e^{\Re(\alpha_B)} |e_A, g_B, \alpha_A, \alpha_B + 1\rangle + \\ & x_4 e^{\Re(\alpha_A)} |g_A, e_B, \alpha_A + 1, \alpha_B\rangle + \\ & x_5 |g_A, g_B, \alpha_A, \alpha_B\rangle \end{aligned} \tag{170}$$

1. $C_{AB}(t)$

Using the same procedure followed in Section III A 1, one could achieve the below result for $Q(t)$:

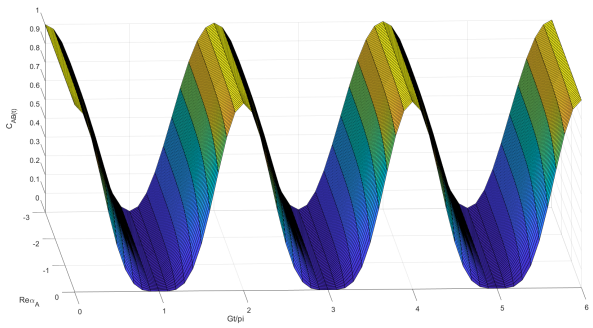

FIG. 12. Zoomed version of the C_{AB} of $|\Phi\rangle$ where $\theta = \pi/4$

$$Q_{AB}(t) = 2|x_1'||x_5'| - 2|x_3'||x_4'| \tag{171}$$

where

$$\begin{aligned}
|x_1'| &= |x_1| = |\cos(\theta)| \cos^2\left(\frac{Gt}{2}\right) \\
|x_5'| &= |x_5| = |\sin(\theta)| \\
|x_3'| &= e^{\Re(\alpha_B)} |\cos(\theta)| \left|\cos\left(\frac{Gt}{2}\right)\right| \left|\sin\left(\frac{Gt}{2}\right)\right| \\
|x_4'| &= e^{\Re(\alpha_A)} |\cos(\theta)| \left|\cos\left(\frac{Gt}{2}\right)\right| \left|\sin\left(\frac{Gt}{2}\right)\right|
\end{aligned} \tag{172}$$

Thus,

$$Q(t) = \cos^2\left(\frac{Gt}{2}\right) \left[|\sin(2\theta)| - 2\sin^2\left(\frac{Gt}{2}\right)\cos^2(\theta) e^{\Re(\alpha_A)+\Re(\alpha_B)}\right] \tag{173}$$

The C_{AB} plot in Fig. 11.(a) shows the similar behaviour to C_{AB} of the one-photon $|\Phi\rangle$ state observed in Section III A. When the α_A and α_B are taken as zero the plot will be the same as one photon case. For α values different than zero the maximum value that the concurrence can take decreases. Moreover, the ESD time shows decrease with more negative $\Re(\alpha)$ values shown in Fig. (12)

2. $C_{ab}(t)$

$$Q(t) = 2|x_2'||x_5'| - 2|x_3'||x_4'| \tag{174}$$

$$\begin{aligned}
Q(t) = \sin^2\left(\frac{Gt}{2}\right) e^{\Re(\alpha_A)+\Re(\alpha_B)} \\
\cdot \left[|\sin(2\theta)| - 2\cos^2\left(\frac{Gt}{2}\right)\cos^2(\theta)\right]
\end{aligned} \tag{175}$$

In Fig. 11.(b), for the higher $\Re(\alpha)$ values, the plot becomes similar to the one-photon case.(see Fig. 4.(b)) Yet, for the negative $\Re(\alpha)$ values, plot shows an apparent exponential decay as expected due to the common exponential term of consisting of the summation of both $\Re(\alpha_A)$ and $\Re(\alpha_B)$ (175).

3. $C_{Ab}(t)$

$$Q(t) = 2|x_3'||x_5'| - 2|x_1'||x_2'| \tag{176}$$

$$\begin{aligned}
Q(t) = \frac{1}{2}\cos^2(\theta)|\sin(Gt)| e^{\Re(\alpha_B)} \\
\cdot \left[2|\tan(\theta)| - e^{\Re(\alpha_A)}|\sin(Gt)|\right]
\end{aligned} \tag{177}$$

In Fig. 11.(c), for the higher $\Re(\alpha)$ values, the plot becomes similar to the one-photon case.(see Fig. 4.(c)) However, for the negative $\Re(\alpha)$ values, plot shows an exponential decay as expected. Yet, this decay is not fast as that of C_{ab}.

4. $C_{aB}(t)$

$$Q(t) = 2|x_4'||x_5'| - 2|x_1'||x_2'| \tag{178}$$

$$\begin{aligned}
Q(t) = \frac{1}{2}\cos^2(\theta)|\sin(Gt)| e^{\Re(\alpha_A)} \\
\cdot \left[2|\tan(\theta)| - e^{\Re(\alpha_B)}|\sin(Gt)|\right]
\end{aligned} \tag{179}$$

Here, it should be noted that Fig. (11) shows the C_{Ab} as equal to the C_{aB}. This is done because of the numerical analysis simplification purposes. For the plots, $\Re(\alpha_A)$ is taken as equal to $\Re(\alpha_B)$. Thus, the Eq. (179) becomes the Eq. (177); even though, in reality, they are different.

5. $C_{Aa}(t)$

$$Q(t) = 2|x_2'x_3' + x_4'x_1'| \tag{180}$$

$$\begin{aligned}
Q(t) = \cos^2(\theta)|\sin(Gt)| e^{\Re(\alpha_A)} \\
\cdot \left[e^{2\Re(\alpha_B)}\sin^2\left(\frac{Gt}{2}\right) + \cos^2\left(\frac{Gt}{2}\right)\right]
\end{aligned} \tag{181}$$

In Fig. 11.(d), for the higher $\Re(\alpha)$ values, the plot becomes similar to the one-photon case.(see Fig. 4.(d)) For the negative $\Re(\alpha)$ values, plot shows an exponential

decay as expected similar to (b) and (c). Comparing plot (d) with the (c), one can say that (d) has faster decay. This is due to the equation inside the parentheses.(177, 181) Since C_{Ab} includes extraction inside the parentheses, decay is expected to be slower.

6. $C_{Bb}(t)$

$$Q(t) = 2|x_2' x_4' + x_3' x_1'| \tag{182}$$

$$Q(t) = \cos^2(\theta)|\sin(Gt)|e^{\Re(\alpha_B)} \cdot \left[e^{2\Re(\alpha_A)} \sin^2\left(\frac{Gt}{2}\right) + \cos^2\left(\frac{Gt}{2}\right)\right] \tag{183}$$

Again here, it should be noted that Fig. (11) shows the C_{Aa} as equal to the C_{Bb}. This is done because of the numerical analysis simplification purposes as mentioned before.

B. Partially Entangled Bell State $|\Psi_{AB}\rangle$

$$|\Psi(0)\rangle = |\Psi_{AB}\rangle \otimes |\alpha_A, \alpha_B\rangle \tag{184}$$

Using the same procedure as the previous section, one can obtain:

$$|\Psi(t)\rangle = x_1' |e_A, g_B, \alpha_A, \alpha_B\rangle + x_2' |g_A, e_B, \alpha_A, \alpha_B\rangle + x_3' |g_A, g_B, \alpha_A + 1, \alpha_B\rangle + x_4' |g_A, g_B, \alpha_A, \alpha_B + 1\rangle \tag{185}$$

where the coefficients are:

$$\begin{aligned} x_1' &= x_1 \\ x_2' &= x_2 \\ x_3' &= x_3 e^{\Re(\alpha_A)} \\ x_4' &= x_4 e^{\Re(\alpha_B)} \end{aligned} \tag{186}$$

Here x_1, x_2, x_3, x_4 are the same coefficients given in Eq. (111). Similar to previous sections $|\Psi\rangle$ state has simpler terms compared to $|\Phi\rangle$.

1. $C_{AB}(t)$

$$C_{AB}(t) = 2|x_1'||x_2'| \tag{187}$$

$$C_{AB}(t) = |\sin(2\theta)| cos^2\left(\frac{Gt}{2}\right) \tag{188}$$

Neither α_A nor α_B dependence for this concurrence is shown in Fig. 13. (a). This is yet an interesting result meaning that even though the cavity is in the coherent state, the amplitude of the coherent state does not affect the entanglement between atoms A and B.

2. $C_{ab}(t)$

$$C_{ab}(t) = 2|x_3'||x_4'| \tag{189}$$

$$C_{ab}(t) = e^{\Re(\alpha_A)+\Re(\alpha_B)}|\sin(2\theta)| \sin^2\left(\frac{Gt}{2}\right) \tag{190}$$

Fig. 13.(b) shows the plot for C_{ab} where the fastest decay occurs compared to the other concurrence as expected due to the exponential term.

3. $C_{Ab}(t)$

$$C_{Ab}(t) = 2|x_1'||x_4'| \tag{191}$$

$$C_{Ab}(t) = \frac{1}{2} e^{\Re(\alpha_B)}|\sin(2\theta)| \sin(Gt)| \tag{192}$$

Fig. 13.(c) shows the plot for C_{Ab}. For the higher values of $\Re(\alpha)$ the concurrence gets similar results to one-photon $|Phi_{AB}\rangle$ initial states.

4. $C_{aB}(t)$

$$C_{aB}(t) = 2|x_2'||x_3'| \tag{193}$$

$$C_{aB}(t) = \frac{1}{2} e^{\Re(\alpha_A)}|\sin(2\theta)| \sin(Gt)| \tag{194}$$

Due to numerical analysis simplifications, $\Re(\alpha_A)$ and $\Re(\alpha_B)$ are taken as same vectors also for the $|\Psi\rangle$ state. Thus, C_{aB} becomes C_{Ab}.

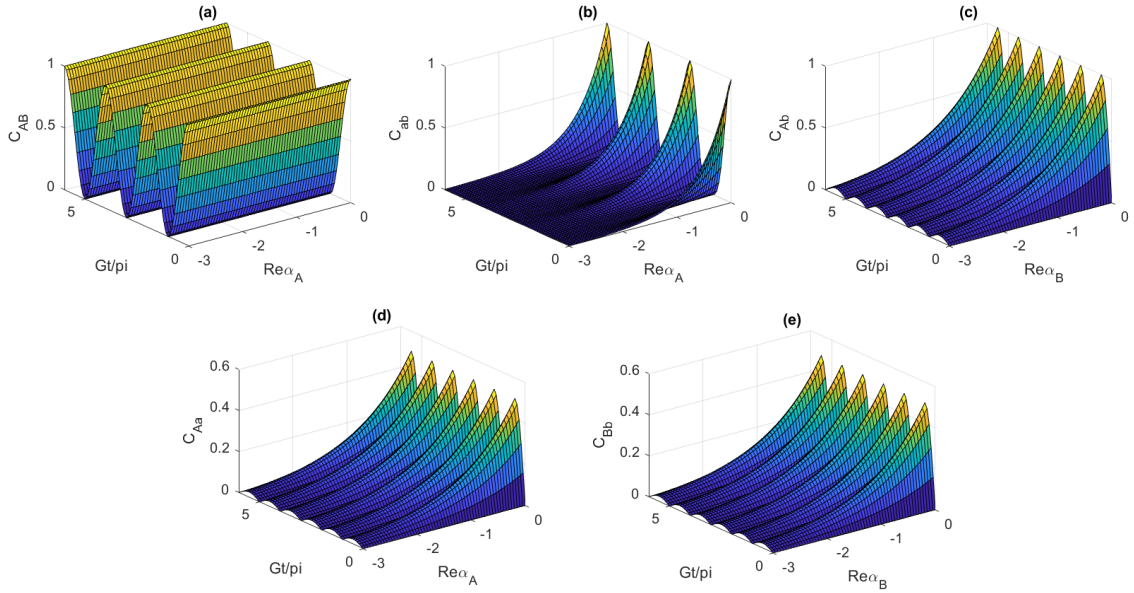

FIG. 13. (a) Plot for C_{AB} of $|\Psi\rangle$ as a function of time and $\Re(\alpha_A)$ where $\theta = \pi/4$. (b) Plot for C_{ab} as a function of time and $\Re(\alpha_A)$ where $\theta = \pi/4$. (c) Plot for C_{Ab} as a function of time and $\Re(\alpha_B)$ where $\theta = \pi/4$. (d) Plot for C_{Aa} as a function of time and $\Re(\alpha_A)$ where $\theta = \pi/4$. (e) Plot for C_{Bb} as a function of time and $\Re(\alpha_B)$ where $\theta = \pi/4$. Similar to other $|\Psi_{AB}\rangle$ initial state cases, C_{aB} is not shown since $C_{aB} = C_{Ab}$.

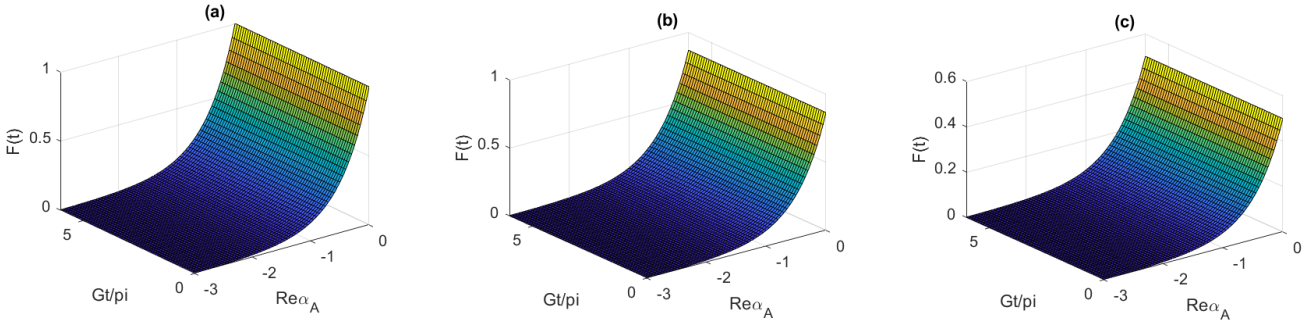

FIG. 14. (a) Entanglement conservation as a function of time and $\Re(\alpha_A)$ where $\theta = \pi/4$. (b) Entanglement conservation a function of time and $\Re(\alpha_A)$ where $\theta = \pi/6$. (c) Entanglement conservation as a function of time and $\Re(\alpha_A)$ where $\theta = \pi/12$.

5. $C_{Aa}(t)$

$$C_{Aa}(t) = 2|x_1'||x_3'| \tag{195}$$

$$C_{Aa}(t) = e^{\Re(\alpha_A)} \cos^2(\theta) |\sin(Gt)| \tag{196}$$

Fig. 13.(d) demonstrates the C_{Aa}. This plot is similar to that of C_{Ab}, yet it has a smaller maximum value which can be also observed in the previous Section III B.

6. $C_{Bb}(t)$

$$C_{Bb}(t) = 2|x_2'||x_4'| \tag{197}$$

$$C_{Bb}(t) = e^{\Re(\alpha_B)} \sin^2(\theta) |\sin(Gt)| \tag{198}$$

Since the plots are only obtained for the $\theta = \pi/4$, it is not a surprise to obtain the same results with C_{Aa}. For the different angle values, the plots will not be the same apparently.

Similar to Section III and IV, one can find a conservation function for the entanglement of the system states

$|\Phi\rangle$ and $|\Psi\rangle$. Here, only for the $|\Psi\rangle$ state, the entanglement conservation function can be found. For that of $|\Phi\rangle$, studies are still continuing. Thus, the conservation function for $|\Psi\rangle$ is:

$$\begin{aligned}F(t) =& e^{\Re(\alpha_A)+\Re(\alpha_B)}C_{AB}(t) + C_{ab}(t) + e^{\Re(\alpha_A)}C_{Ab}(t) - \\ & e^{\Re(\alpha_B)}C_{aB}(t) + e^{\Re(\alpha_B)}\sin^2(\theta)C_{Aa}(t) - \\ & e^{\Re(\alpha_A)}\cos^2(\theta)C_{Bb}(t) = \\ & |\sin(2\theta)|e^{\Re(\alpha_A)+\Re(\alpha_B)}\end{aligned} \tag{199}$$

As expected there is a contribution coming from the exponential term of the $\Re(\alpha_A)$ and $\Re(\alpha_B)$. Similar to the conservation equation (128), the conservation equation (199) includes the $|\sin(2\theta)|$ in addition to the exponential term. Fig. 14 shows the entanglement conservation function for three different initial angle values in terms of time and $\Re(\alpha)$. The figure demonstrates that there is no dependence on time for all three cases. Yet decreasing the $\Re(\alpha)$ values yields smaller maximum values and exponential decay.

VI. MIXED INITIAL STATE CASE

This section examines another type of initial state which is a mixed initial state. Here, the mixed state is taken in the X form. (68). And the system is the same model used in the Section III. Meaning inside the cavity one photon transition between the atom and the cavity is allowed.

$$\rho^{AB}(0) = \frac{1}{3}\begin{bmatrix}1&0&0&0\\0&1&1&0\\0&1&1&0\\0&0&0&0\end{bmatrix} \tag{200}$$

$$\rho_{sys}(0) = \rho_{AB}(0) \otimes |0_a, 0_b\rangle \langle 0_a, 0_b| \tag{201}$$

Firstly, one can write the density matrix in terms of the basis $\{|e,e\rangle, |e,g\rangle, |g,e\rangle, |g,g\rangle\}$ to find the time evolution of the ρ_{sys}. Thus, the matrix (215) can be written as:

$$\begin{aligned}\rho_{AB}(0) =& \frac{1}{3}|e_A, e_B\rangle\langle e_A, e_B| + \frac{1}{3}|e_A, g_B\rangle\langle e_A, g_B| + \\ & \frac{1}{3}|g_A, e_B\rangle\langle e_A, g_B| + \frac{1}{3}|e_A, g_B\rangle\langle g_A, e_B| + \\ & \frac{1}{3}|g_A, e_B\rangle\langle g_A, e_B|\end{aligned} \tag{202}$$

The density matrix describing the given mixed state:

$$\rho_{AB}(0) = \sum p_i |\overline{\Psi}_i(0)\rangle\langle\overline{\Psi}_i(0)| \tag{203}$$

$$\begin{aligned}|\overline{\Psi}_1(0)\rangle &= |e_A, e_B\rangle, \quad p_1 = \frac{1}{3} \\ |\overline{\Psi}_2(0)\rangle &= \frac{1}{\sqrt{2}}\left(|e_A, g_B\rangle + |g_A, e_B\rangle\right), \quad p_2 = \frac{2}{3}\end{aligned} \tag{204}$$

These two initial states can be written in terms of partially entangled states $|\Phi_{AB}\rangle$ and $|\Psi_{AB}\rangle$ respectively.

Using the initial state Eq. (66) of $|\Phi_{AB}\rangle$ for $\alpha = 0$, the atom-cavity system can be written as $|\Psi_1\rangle$:

$$\begin{aligned}|\overline{\Psi}_1(0)\rangle &= |\Phi_{AB}\rangle = |e_A, e_B\rangle \\ |\Psi_1(0)\rangle &= |\overline{\Psi}_1(0)\rangle \otimes |0_a, 0_b\rangle\end{aligned} \tag{205}$$

Using the same procedure followed in Section III A one can find the time evolution of $|\Psi_1(t)\rangle$ as:

$$\begin{aligned}|\Psi_1(t)\rangle =& x_1|e_A, e_B, 0_a, 0_b\rangle + x_2|g_A, g_B, 1_a, 1_b\rangle + \\ & x_3|e_A, g_B, 0_a, 1_b\rangle + x_4|g_A, e_B, 1_a, 0_b\rangle + \\ & x_5|g_A, g_B, 0_a, 0_b\rangle\end{aligned} \tag{206}$$

Here the coefficients can be written as below where $\cos(\alpha) = 1$ and $\sin(\alpha) = 0$:

$$\begin{aligned}&x_1 = (Le^{-i\lambda^+ t} + Me^{-i\lambda^- t})^2, \\ &x_2 = (\sqrt{LM}e^{-i\lambda^+ t} - \sqrt{LM}e^{-i\lambda^- t})^2, \\ &x_3 = (Le^{-i\lambda^+ t} + Me^{-i\lambda^- t})(\sqrt{LM}e^{-i\lambda^+ t} - \sqrt{LM}e^{-i\lambda^- t}), \\ &x_4 = x_3, \\ &x_5 = 0 \\ &\text{for} \quad \Delta = 0 \quad L = M = \frac{1}{2}\end{aligned} \tag{207}$$

The absolute value of coefficients of $|\Psi_1(t)\rangle$ can be written as below in which the global phase factor is ignored (Eq. (91)).

$$\begin{aligned}|x_1| &= \cos^2\left(\frac{Gt}{2}\right) \\ |x_2| &= \sin^2\left(\frac{Gt}{2}\right) \\ |x_3| &= \frac{1}{2}|\sin(Gt)| \\ |x_4| &= |x_3|\end{aligned} \tag{208}$$

The second pure state constitutes the mixed state can be written by using the initial state Eq. (67) of $|\Psi_{AB}\rangle$ for $\alpha = \pi/4$:

$$\begin{aligned}|\overline{\Psi}_2(0)\rangle &= |\Phi_{AB}\rangle = \frac{1}{\sqrt{2}}|e_A, g_B\rangle + \frac{1}{\sqrt{2}}|g_A, e_B\rangle \\ |\Psi_2(0)\rangle &= |\overline{\Psi}_2(0)\rangle \otimes |0_a, 0_b\rangle\end{aligned} \tag{209}$$

Using the same procedure followed in Section III B one can find the time evolution of $|\Psi_2(t)\rangle$ as:

$$|\Psi_2(t)\rangle = x'_1 |e_A, g_B, 0_a, 0_b\rangle + x'_2 |g_A, e_B, 0_a, 0_b\rangle + x'_3 |g_A, g_B, 1_a, 0_b\rangle + x'_4 |g_A, g_B, 0_a, 1_b\rangle \quad (210)$$

Here the coefficients can be written as below where $\cos(\alpha) = \frac{1}{\sqrt{2}}$ and $\sin(\alpha) = \frac{1}{\sqrt{2}}$:

$$\begin{aligned} x'_1 &= \frac{1}{\sqrt{2}}(Le^{-i\lambda^+ t} + Me^{-i\lambda^- t}) \\ x'_2 &= \frac{1}{\sqrt{2}}(Le^{-i\lambda^+ t} + Me^{-i\lambda^- t}) \\ x'_3 &= \frac{1}{\sqrt{2}}(\sqrt{LM}e^{-i\lambda^+ t} - \sqrt{LM}e^{-i\lambda^- t}) \\ x'_4 &= \frac{1}{\sqrt{2}}(\sqrt{LM}e^{-i\lambda^+ t} - \sqrt{LM}e^{-i\lambda^- t}) \\ \text{for} \quad \Delta = 0 \quad & L = M = \frac{1}{2} \end{aligned} \quad (211)$$

The absolute value of coefficients of $|\Psi_1(t)\rangle$ can be written as below:

$$\begin{aligned} |x'_1| &= \frac{1}{\sqrt{2}} \left|\cos\left(\frac{Gt}{2}\right)\right| \\ |x'_2| &= |x'_1| \\ |x'_3| &= \frac{1}{\sqrt{2}} \left|\sin\left(\frac{Gt}{2}\right)\right| \\ |x'_4| &= |x'_3| \end{aligned} \quad (212)$$

The final time-evolved density matrix can be written as the sum of the pure states found above.

$$\rho_{sys}(t) = \frac{1}{3} |\Psi_1(t)\rangle \langle\Psi_1(t)| + \frac{2}{3} |\Psi_2(t)\rangle \langle\Psi_2(t)| \quad (213)$$

A. C_{AB}

Similar to previous sections, one should obtain the related reduced density matrix to find the concurrence.

$$\rho_{AB}(t) = Tr_{ab}[\rho_{sys}(t)]$$

$$\begin{aligned} \rho_{AB}(t) &= \frac{1}{3} Tr_{ab}[|\Psi_1(t)\rangle \langle\Psi_1(t)|] + \frac{2}{3} Tr_{ab}[|\Psi_2(t)\rangle \langle\Psi_2(t)|] \\ \rho_{AB1} &= Tr_{ab}[|\Psi_1(t)\rangle \langle\Psi_1(t)|] \\ \rho_{AB2} &= Tr_{ab}[|\Psi_2(t)\rangle \langle\Psi_2(t)|] \end{aligned} \quad (214)$$

$$\rho^{AB}(t) = \begin{bmatrix} a(t) & 0 & 0 & w(t) \\ 0 & b(t) & z(t) & 0 \\ 0 & z^*(t) & c(t) & 0 \\ w^*(t) & 0 & 0 & d(t) \end{bmatrix} \quad (215)$$

For all concurrences, the reduced density matrices are in the X form. Therefore, all the coefficients are written in terms of $a(t), b(t), c(t), d(t), w(t), w^*(t), z(t), z^*(t)$. Moreover, the reduced density matrix is calculated using the ρ_{AB1} and ρ_{AB2} which are calculated in the previous section III.

$$\begin{aligned} a(t) &= \frac{1}{3}|x_1|^2 \\ b(t) &= \frac{1}{3}|x_3|^2 + \frac{2}{3}|x'_1|^2 \\ c(t) &= \frac{1}{3}|x_4|^2 + \frac{2}{3}|x'_2|^2 \\ d(t) &= \frac{1}{3}|x_2|^2 + \frac{2}{3}(|x'_3|^2 + |x'_4|^2) \\ z(t) &= \frac{2}{3}x'^*_1 x'_2 \\ z^*(t) &= \frac{2}{3}x'_1 x^*_2 \\ w(t) &= w^*(t) = 0 \end{aligned} \quad (216)$$

$$C(\rho) = max[0, Q(t)] = 2max[0, |z| - \sqrt{ad}]$$

From the Fig. (15), one can observe that for C_{AB} ESD occurs. In the previous section, ESD only occurs in the $|\Phi\rangle$ state. Yet, ESD does not occur only for the C_{AB} of this mixed state.

B. $C_{ab}(t)$

$$\rho_{ab}(t) = Tr_{AB}[\rho_{sys}(t)]$$

$$\begin{aligned} a(t) &= \frac{1}{3}|x_1|^2 + \frac{2}{3}(|x'_1|^2 + |x'_2|^2) \\ b(t) &= \frac{1}{3}|x_3|^2 + \frac{2}{3}|x'_4|^2 \\ c(t) &= \frac{1}{3}|x_4|^2 + \frac{2}{3}|x'_3|^2 \\ d(t) &= \frac{1}{3}|x_2|^2 \\ z(t) &= \frac{2}{3}x'^*_3 x'_4 \\ z^*(t) &= \frac{2}{3}x'_3 x^*_4 \\ w(t) &= w^*(t) = 0 \end{aligned} \quad (217)$$

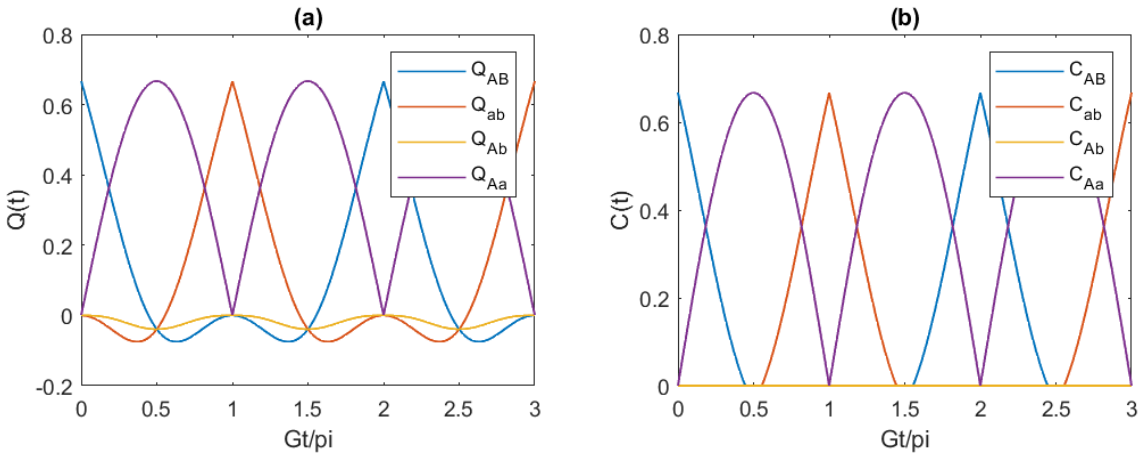

FIG. 15. (a) Q function for the pairwise cases AB, ab, Ab and Aa respectively. (b) Concurrences for the given pairwises

C_{AB} and C_{ab} shows similar aspects with Section III. Such as, the C_{ab} is the π/G phase-lagged version of the C_{AB}.

C. $C_{Ab}(t)$

$$\rho_{Ab}(t) = Tr_{aB}[\rho_{sys}(t)]$$

$$\begin{aligned}
a(t) &= \frac{1}{3}|x_4|^2 + \frac{2}{3}(|x_3'|^2 + |x_2'|^2) \\
b(t) &= \frac{1}{3}|x_2|^2 + \frac{2}{3}|x_4'|^2 \\
c(t) &= \frac{1}{3}|x_1|^2 + \frac{2}{3}|x_1'|^2 \\
d(t) &= \frac{1}{3}|x_3|^2 \\
z(t) &= \frac{2}{3}x_1'^* x_4' \\
z^*(t) &= \frac{2}{3}x_1' x_4^* \\
w(t) &= w^*(t) = 0
\end{aligned} \tag{218}$$

For the concurrence, the part coming from the $|\Psi_1(t)\rangle$ is always less than or equal to zero since it is not an entangled state initially. (205) The contribution of these negative values is more than the effect of the C_{Ab} of $|\Psi_2(t)\rangle$. Thus, intuitively, the negative results for Q_{Ab} are not unprecedented.

D. $C_{aB}(t)$

Due to the symmetry mentioned in Sections (III A) and (III B) one can directly say that $C_{aB}(t)$ and $C_{Ab}(t)$ are equal.

E. $C_{Aa}(t)$

$$\rho_{Aa}(t) = Tr_{Bb}[\rho_{sys}(t)]$$

Since in $\rho_{Aa}(t)$ density matrix $d(t) = 0$ and $w(t) = 0$, it is sufficient to write the $z(t)$ coefficient only.

$$z(t) = \frac{1}{3}(x_2 x_3^* + x_4 x_1^*) + \frac{2}{3}x_1'^* x_3' \tag{219}$$

$$C_{Aa}(t) = 2|z| \tag{220}$$

If the global phase factor is ignored, one can accept the coefficients as real factors.

$$\begin{aligned}
|z| &= \left|\frac{1}{3}(x_2 x_3 + x_4 x_1) + \frac{2}{3}x_1' x_3'\right| \\
&= \left|\frac{1}{3}x_3(x_1 + x_2) + \frac{2}{3}x_1' x_3'\right| \\
&= \left|\frac{1}{3}\frac{1}{2}\sin(Gt) + \frac{2}{3}\frac{1}{2}\sin\left(\frac{Gt}{2}\right)\cos\left(\frac{Gt}{2}\right)\right| \\
&= \frac{1}{3}|\sin(Gt)|
\end{aligned} \tag{221}$$

F. $C_{Bb}(t)$

$$\rho_{Bb}(t) = Tr_{Aa}[\rho_{sys}(t)]$$

$$\begin{aligned}
z &= \frac{1}{3}(x_2 x_3^* + x_4 x_1^*) + \frac{2}{3}x_2'^* x_4' \\
|z| &= \left|\frac{1}{3}(x_2 x_3 + x_4 x_1) + \frac{2}{3}x_1' x_4'\right|
\end{aligned} \tag{222}$$

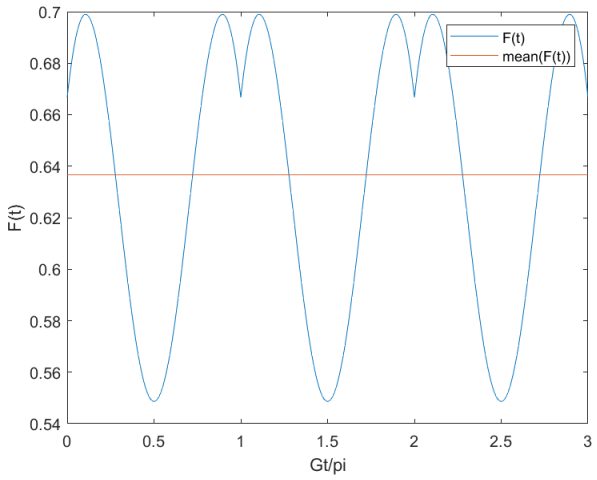

FIG. 16. Entanglement conservation function and its mean value plot for the initial mixed state

Since $x'_4 = x'_3$ the result is the same as $C_{Aa}(t)$.

Observing Fig.(15), one can deduce that there is some entanglement conservation. The sum of the four concurrences given in the plot seems to be plausible for the conservation relation. When these concurrences are summed directly, Fig. (16) is obtained. From this figure, it can be understood that it is time-dependent yet the amplitude of the sum function F(t) oscillates between a small interval between 0.56 to 0.7. Its mean is calculated as nearly 0.64. It can be a logical result if the final conserved quantity is anticipated as a summation of the mixed states like:

$$F(t) = |\sin(2\alpha_1)|p_1 + |\sin(2\alpha_2)|p_2 \tag{223}$$

$$F(t) = |\sin(2\times 0)|\frac{1}{3} + |\sin(2\frac{\pi}{4})|\frac{2}{3} = \frac{2}{3} \tag{224}$$

where the anticipated result is quite close to the result obtained from the summation of the four concurrences. Moreover, for this initial state matrix, in [4], there is no rebirth occurring. This arises from the cavity modes. In that article, the cavity is assumed to be an infinite mode cavity meaning that all frequencies affect the atom inside the cavity.

VII. TWO MODES CAVITY

In this section, the single-mode cavity is changed to a two-modes cavity in which the cavity can interact with two frequencies being $\omega 1$ and $\omega 2$. The motivation behind investigating the two-mode case is to understand the effects of the number of cavity modes on the concurrences. In [4] and [9], it is mentioned that if a larger number of cavity modes would be provided, a longer time would be needed for a rebirth to occur, and as a limiting case, if the number of modes is infinite, the quantum correlation can not rebirth in any finite time. Similar to JC model used in the single-mode cavity, the new Hamiltonian can be written as:

TABLE I. Eigenstates and the eigenvalue of the two modes field cavity and the atom system.

Eigenstates	Eigenvalue
$\|g, n_1, n_2\rangle$	
$\|e, n_1, n_2 - 1\rangle$	$n_1 + n_2$
$\|e, n_1 - 1, n_2\rangle$	

$$H_{tot} = H_{at} + H_{cav} + H_{int} \tag{225}$$

where

$$\begin{aligned} H_{at} &= \frac{1}{2}\omega_A \sigma_Z^A, \\ H_{cav} &= \omega_1 \hat{a_1}^\dagger \hat{a_1} + \omega_2 \hat{a_2}^\dagger \hat{a_2} \\ H_{int} &= g_1(\sigma_-^A \hat{a_1}^+ + \sigma_+^A \hat{a_1}) + g_2(\sigma_-^A \hat{a_2}^+ + \sigma_+^A \hat{a_2}) \end{aligned} \tag{226}$$

The differences between single-mode Hamiltonian (52) and the two-modes Hamiltonian (226) are the additional terms $\omega_2 \hat{a_2}^\dagger \hat{a_2}$ and $g_2(\sigma_-^A \hat{a_2}^+ + \sigma_+^A \hat{a_2})$, which are the terms coming from the second radiation field. Again, the same procedure is followed in Section III and an operator is described which is the number of excitation:

$$\hat{N}_{exc} = \hat{a_1}^\dagger \hat{a_1} + \hat{a_2}^\dagger \hat{a_2} + \sigma_+ \sigma_- \tag{227}$$

This number of excitation operator commutes with the Hamiltonian (226):

$$[\hat{H}, \hat{N}_{exc}] = 0 \tag{228}$$

Thus, the eigenstates of the number of excitation operator and the two-modes Hamiltonian are the same which are shown in Table I.

$$\hat{H} = \bigoplus_{n_1+n_2=0}^{\infty} H^{(n_1+n_2)} \tag{229}$$

It should also be noted that the Hamiltonian is a $\infty \times \infty$ matrix in a block structure. For each eigenvalue (number of photons inside the cavity), there exists 3×3 block matrix in the Hamiltonian. However, for the $n_1 + n_2 = 0$ case there is only one element being correspond to the $|g, 0, 0\rangle$. Moreover, for the case $n_1 + n_2 = 1$ the block matrix will be in the 2×2 not 3×3. The Hamiltonian for this 2×2 block can be described as:

$$\hat{H}^{(1)} = \begin{bmatrix} A & X \\ X & B \end{bmatrix} \tag{230}$$

For $n_1 = 0$ and $n_2 = 1$ the basis becomes $\{|g,0,1\rangle, |e,0,0\rangle\}$. Whereas for $n_1 = 1$ and $n_2 = 0$ the basis becomes $\{|g,1,0\rangle, |e,0,0\rangle\}$.

$$A = \langle g,0,1|\, \hat{H}\, |g,0,1\rangle = -\frac{\omega_A}{2} + \omega_2, \tag{231}$$

$$B = \langle e,0,0|\, \hat{H}\, |e,0,0\rangle = \frac{\omega_A}{2}, \tag{232}$$

$$X = \langle g,0,1|\, \hat{H}\, |e,0,0\rangle = g_2\sqrt{1} = g_2 \tag{233}$$

Thus,

$$\hat{H}^{(1)} = \begin{bmatrix} -\frac{\omega_A}{2} + \omega_2 & g_2 \\ g_2 & \frac{\omega_A}{2} \end{bmatrix} \text{for } n_1 = 0, n_2 = 1 \tag{234}$$

$$\hat{H}^{(1)} = \begin{bmatrix} -\frac{\omega_A}{2} + \omega_1 & g_1 \\ g_1 & \frac{\omega_A}{2} \end{bmatrix} \text{for } n_1 = 1, n_2 = 0 \tag{235}$$

where eigenvalues are

$$\lambda_1^{\pm} = -\frac{\omega_1}{2} \pm \sqrt{\Delta^2 + G_1^2}, \quad \Delta = \omega_1 - \omega_A, \quad G_1 = 2g_1 \tag{236}$$

$$\lambda_2^{\pm} = -\frac{\omega_2}{2} \pm \sqrt{\Delta^2 + G_2^2}, \quad \Delta = \omega_2 - \omega_A, \quad G_2 = 2g_2 \tag{237}$$

Likewise in Section III, the eigenkets for $n_1 = 0, n_2 = 1$ can be shown as:

$$|\psi_1^+\rangle = c\,|e,0,0\rangle + s\,|g,0,1\rangle \tag{238}$$

$$|\psi_1^-\rangle = -s\,|e,0,0\rangle + c\,|g,0,1\rangle \tag{239}$$

$$c = \cos\left(\frac{\Theta}{2}\right) \quad s = \sin\left(\frac{\Theta}{2}\right) \tag{240}$$

where,

$$\cos(\Theta) = \frac{\Delta}{\sqrt{\Delta^2 + G_2^2}} \quad \sin(\Theta) = \frac{G_2}{\sqrt{\Delta^2 + G_2^2}} \tag{241}$$

Moreover, bare basis can be written in terms of the dressed states:

$$|g,0,0\rangle = |\Psi_0\rangle \tag{242}$$

$$|e,0,0\rangle = c\,|\Psi_1^+\rangle - s\,|\Psi_1^-\rangle \tag{243}$$

$$|g,0,1\rangle = s\,|\Psi_1^+\rangle + c\,|\Psi_1^-\rangle \tag{244}$$

Describing these fundamental terms, the new Hamiltonian for the two two-level atoms and cavities can be introduced as: (see Fig. 2)

$$\begin{aligned} H_{at} &= \frac{1}{2}\omega_A\sigma_Z^A + \frac{1}{2}\omega_B\sigma_Z^B, \\ H_{cav} &= \sum_1^2 \omega_k \hat{a}_k^\dagger \hat{a} + \sum_1^2 \nu_k \hat{b}_k^\dagger \hat{b} \\ H_{int} &= \sum_1^2 (g_k\sigma_-^A\hat{a}_k^\dagger + g_k\sigma_+^A\hat{a}_k) + \sum_1^2 (f_k\sigma_-^B\hat{b}_k^\dagger + f_k\sigma_+^B\hat{b}_k) \end{aligned} \tag{245}$$

Using the new Hamiltonian and the new initial state given below concurrence dynamics can be examined:

$$|\Phi(0)\rangle = |\Phi_{AB}\rangle \otimes |0_{a1}, 0_{a_2}, 0_{b1}, 0_{b_2}\rangle \tag{246}$$

where (a_1, a_2) and (b_1, b_2) refer to the two modes of the cavity a and b respectively. Expanding the above equation:

$$\begin{aligned} |\Phi(0)\rangle = (\cos(\alpha)\,|e_A, e_B\rangle + \sin(\alpha)\,|g_A, g_B\rangle) \otimes \\ |0_{a_1}, 0_{a_2}, 0_{b_1}, 0_{b_2}\rangle \end{aligned} \tag{247}$$

$$\begin{aligned} |\Phi(0)\rangle = \cos(\alpha)\,|e_A, 0_{a_1}, 0_{a_2}\rangle \otimes |e_B, 0_{b_1}, 0_{b_2}\rangle + \\ \sin(\alpha)\,|g_A, 0_{a_1}, 0_{a_2}\rangle \otimes |g_B, 0_{b_1}, 0_{b_2}\rangle \end{aligned} \tag{248}$$

Applying the same procedure used in Section III A, one can achieve the time-evolved system of the $|\Phi\rangle$ as:

$$\begin{aligned} |\Phi(t)\rangle = & x_1\,|e_A, e_B, 0_{a_1}, 0_{a_2}, 0_{b_1}, 0_{b_2}\rangle + \\ & x_2\,|g_A, g_B, 0_{a1}, 1_{a_2}, 0_{b_1}, 1_{b_2}\rangle + \\ & x_3\,|e_A, g_B, 0_{a_1}, 0_{a_2}, 0_{b_1}, 1_{b_2}\rangle + \\ & x_4\,|g_A, e_B, 0_{a_1}, 1_{a_2}, 0_{b_1}, 0_{b_2}\rangle + \\ & x_5\,|g_A, g_B, 0_{a_1}, 0_{a_2}, 0_{b_1}, 0_{b_2}\rangle \end{aligned} \tag{249}$$

where x coefficients are the same as Eq.(85). From these results, one can deduce that the concurrences will be the same as the single-mode cavity case at Section III A even though they have different eigenvalues and different numbers of modes. To understand the reasoning behind this, Eq.(91) should be seen. The detuning is zero, since the system is assumed to be in resonance. Thus before the $\pm$ part of the eigenvalue equation (237) becomes the global phase. The only effecting part is the remaining G_2 term yielding the same concurrence between the single-mode $|\Phi\rangle$ in the previous sections. Thus, the frequency and the ESD time of the concurrences depend on the coupling factor. The same procedure can be applied to the $|\Psi\rangle$ states. It should be noted that, while finding the concurrences, the partial trace of the system density matrix should be taken in terms of all the field modes.

Now, consider the 3×3 block Hamiltonian for the number of photons greater than 1.

$$\hat{H}^{(n_1+n_2)} = \begin{bmatrix} A & X & Y \\ X & B & 0 \\ Y & 0 & C \end{bmatrix} \tag{250}$$

Here, eigenstates given in Table I create the basis for the Hamiltonian. Each term inside this block can be found as:

$$
\begin{aligned}
A &= \langle g, n_1, n_2 | \hat{H} | g, n_1, n_2 \rangle = -\frac{1}{2}\omega_A + \omega_1 n_1 + \omega_2 n_2, \\
B &= \langle e, n_1 - 1, n_2 | \hat{H} | e, n_1 - 1, n_2 \rangle \\
&= \frac{1}{2}\omega_A + \omega_1 (n_1 - 1) + \omega_2 n_2, \\
C &= \langle e, n_1, n_2 - 1 | \hat{H} | e, n_1, n_2 - 1 \rangle \\
&= \frac{1}{2}\omega_A + \omega_1 n_1 + \omega_2 (n_2 - 1), \\
X &= \langle g, n_1, n_2 | \hat{H} | e, n_1 - 1, n_2 \rangle = g_1 \sqrt{n_1}, \\
Y &= \langle g, n_1, n_2 | \hat{H} | e, n_1, n_2 - 1 \rangle = g_2 \sqrt{n_2}
\end{aligned} \tag{251}
$$

To find the eigenvalues of (250), the matrix is diagonalized and the characteristic polynomial is found as:

$$
\begin{aligned}
&\lambda^3 - (A + B + C)\lambda^2 + (AB + BC + AC - Y^2 - X^2)\lambda \\
&(BY^2 + CX^2 - ABC) = 0
\end{aligned} \tag{252}
$$

The general solution for the general cubic formula for $ax^3 + bx^2 + cx + d = 0$:

$$
\begin{aligned}
&\Delta_0 = b^2 - 3ac \\
&\Delta_1 = 2b^3 - 9abc + 27a^2 d \\
&C = \sqrt[3]{\frac{\Delta_1 \pm \sqrt{\Delta_1^2 - 4\Delta_0^3}}{2}} \\
&\lambda_k = -\frac{1}{3}\left(b + \xi^k C + \frac{\Delta_0}{\xi^k C}\right), \quad k \in \{0, 1, 2\}, \xi = \frac{-1 + \sqrt{3}i}{2}
\end{aligned} \tag{253}
$$

Thus, $\lambda_0, \lambda_1, \lambda_2$ are the eigenvalues of the (226). Similar to 2×2 block version the dressed states can be written in terms of the eigenstates of the number of excitation operator:

$$
|\Psi_n^+\rangle = a_1 |g, n_1, n_2\rangle + a_2 |e, n_1, n_2 - 1\rangle + a_3 |e, n_1 - 1, n_2\rangle \tag{254}
$$

$$
|\Psi_n^0\rangle = b_1 |g, n_1, n_2\rangle + b_2 |e, n_1, n_2 - 1\rangle + b_3 |e, n_1 - 1, n_2\rangle \tag{255}
$$

$$
|\Psi_n^-\rangle = c_1 |g, n_1, n_2\rangle + c_2 |e, n_1, n_2 - 1\rangle + c_3 |e, n_1 - 1, n_2\rangle \tag{256}
$$

Fig. (17) demonstrates the eigenstates of the Hamiltonian (226).

Assuming that the two photons exist inside the cavity accepting $n_1 = 1$ and $n_2 = 1$. Eigenstates of the system can be shown as:

$$
|\Psi_2^+\rangle = a_0 |g, 1, 1\rangle + a_1 |e, 1, 0\rangle + a_2 |e, 0, 1\rangle \tag{257}
$$

$$
|\Psi_2^0\rangle = b_0 |g, 1, 1\rangle + b_1 |e, 1, 0\rangle + b_2 |e, 0, 1\rangle \tag{258}
$$

$$
|\Psi_2^-\rangle = c_0 |g, 1, 1\rangle + c_1 |e, 1, 0\rangle + c_2 |e, 0, 1\rangle \tag{259}
$$

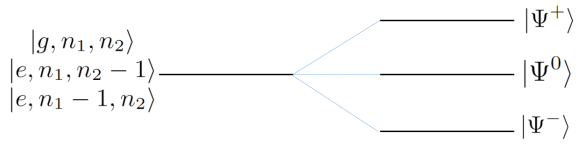

FIG. 17. The degenerate energy states splitting into three eigen-energy levels being $|\Psi^+\rangle$, $|\Psi^0\rangle$, $|\Psi^-\rangle$.

Consider an initial state as:

$$
|\Phi(0)\rangle = |\Phi_{AB}\rangle \otimes |0_{a1}, 1_{a2}, 0_{b1}, 0_{b2}\rangle \tag{260}
$$

which can be expanded as:

$$
\begin{aligned}
|\Phi(0)\rangle = &\cos(\alpha) |e_A, 0_{a1}, 1_{a2}\rangle \otimes |e_B, 0_{b1}, 1_{b2}\rangle \\
&+ \sin(\alpha) |g_A, 0_{a1}, 1_{a2}\rangle \otimes |g_B, 0_{b1}, 1_{b2}\rangle
\end{aligned} \tag{261}
$$

where bare basis can be written in terms of the dressed states:

$$
|e, 0, 1\rangle = x_0 |\Psi_2^+\rangle + x_1 |\Psi_2^0\rangle + x_2 |\Psi_2^-\rangle \tag{262}
$$

$|g, 0, 1\rangle$ is already given above in Eq. (244). Using these expressions,

$$
\begin{aligned}
|\Phi(0)\rangle = &\cos(\alpha)(x_0 |\Psi_2^+\rangle_A + x_1 |\Psi_2^0\rangle_A + x_2 |\Psi_2^-\rangle_A) \otimes \\
&(x_0 |\Psi_2^+\rangle_B + x_1 |\Psi_2^0\rangle_B + x_2 |\Psi_2^-\rangle_B) + \\
&\sin(\alpha)(s |\Psi_1^+\rangle_A + c |\Psi_1^-\rangle_A) \otimes \\
&(s |\Psi_1^+\rangle_B + c |\Psi_1^-\rangle_B)
\end{aligned} \tag{263}
$$

Time evolved $|\Phi\rangle$ can be expressed as:

$$
\begin{aligned}
|\Psi(t)\rangle = &\cos(\alpha)[V |g_A, 1_{a1}, 1_{a2}\rangle + Y |e_A, 1_{a1}, 0_{a2}\rangle \\
&+ Z |e_A, 0_{a1}, 1_{a2}\rangle] \otimes [V |g_B, 1_{b1}, 1_{b2}\rangle + Y |e_B, 1_{b1}, 0_{b2}\rangle \\
&+ Z |e_B, 0_{b1}, 1_{b2}\rangle] + \sin(\alpha)(D |e_A, 0_{a1}, 0_{a2}\rangle \\
&+ E |g_A, 0_{a1}, 1_{a2}\rangle) \otimes (D |e_B, 0_{b1}, 0_{b2}\rangle \\
&+ E |g_B, 0_{b1}, 1_{b2}\rangle)
\end{aligned} \tag{264}
$$

where

$$
\begin{aligned}
V &= x_0 e^{-i\lambda_0 t} a_0 + x_1 e^{-i\lambda_1 t} b_0 + x_2 e^{-i\lambda_2 t} c_0 \\
Y &= x_0 e^{-i\lambda_0 t} a_1 + x_1 e^{-i\lambda_1 t} b_1 + x_2 e^{-i\lambda_2 t} c_1 \\
Z &= x_0 e^{-i\lambda_0 t} a_2 + x_1 e^{-i\lambda_1 t} b_2 + x_2 e^{-i\lambda_2 t} c_2 \\
D &= \sqrt{x_1} \\
E &= \sqrt{x_2}
\end{aligned} \tag{265}
$$

$$
\begin{aligned}
|\Phi(t)\rangle = & X_0 |g,1,1,g,1,1\rangle + X_1 |g,1,1,e,1,0\rangle \\
& + X_2 |g,1,1,e,0,1\rangle + X_3 |e,1,0,g,1,1\rangle \\
& + X_4 |e,1,0,e,1,0\rangle + X_5 |e,1,0,e,0,1\rangle \\
& + X_6 |e,0,1,g,1,1\rangle + X_7 |e,0,1,e,1,0\rangle \\
& + X_8 |e,0,1,e,0,1\rangle + X_9 |e,0,0,e,0,0\rangle \\
& + X_{10} |e,0,0,g,0,1\rangle + X_{11} |g,0,1,e,0,0\rangle \\
& + X_{12} |g,0,1,g,0,1\rangle
\end{aligned} \tag{266}
$$

As can be seen from Eq. (266), there are thirteen states, this is due to the fact that $|e,0,1\rangle$ state which is an eigenket of the 3×3 block Hamiltonian can be defined using three eigenstates. From the tensor product of the system Aa and Bb nine terms occurs. Whereas, $|g,0,1\rangle$ is an eigenstate of the 2×2 block Hamiltonian and can be described with two eigenstates yielding four terms in the equation. The reduced density matrix to find the concurrence C_{AB} can be written as:

$$
\rho_{AB} = Tr_{a_1,a_2,b_1,b_2} \left[|\Phi(t)\rangle \langle \Phi(t)| \right] \tag{267}
$$

Reduce density matrix can be written as in the X form (Eq.(68)) where a, b, c, d, w, w^* shows the components of the X matrix:

$$
\begin{aligned}
a &= |X_4|^2 + |X_5|^2 + |X_7|^2 + |X_8|^2 + |X_9|^2 \\
b &= |X_3|^2 + |X_6|^2 + |X_{10}|^2 \\
c &= |X_1|^2 + |X_2|^2 + |X_{11}|^2 \\
d &= |X_0|^2 + |X_{12}|^2 \\
w &= X_8 X_{12}^* \\
w^* &= X_8^* X_{12}
\end{aligned} \tag{268}
$$

Using the concurrence relation given in (69), $Q(t)$ can be written as:

$$
\begin{aligned}
Q(t) &= 2[|w| - \sqrt{bc}] \\
&= 2[|X_8||X_{12}| - \sqrt{\left(|X_3|^2 + |X_6|^2 + |X_{10}|^2\right) \cdot} \\
&\quad \left(|X_1|^2 + |X_2|^2 + |X_{11}|^2\right)]
\end{aligned} \tag{269}
$$

The concurrence equation (269) shows that the concurrence is not the same as the previous states. Most probably, these results yield higher ESD and period time. However, it is not shown numerically yet. For later studies, this behavior can be investigated in detail also for the other concurrences and partially Bell states.

VIII. CONCLUSION

In this paper, firstly the qubit disentanglement and decoherence are examined through a stochastical model given by Yu and Eberly [1] representing a realistic situation. The decoherence process is investigated using several quantum channels expressed by Kraus operators to understand the effects of both local and mixed dephasing. Whereas, for the entanglement decay, the Wootter concurrence is used. [5] For this realistic noisy model, the entanglement decays can be completely destroyed in a finite time which is shorter than the local and mixed dephasing times. Meaning, the loss of entanglement does not imply complete decoherence. In the following section, another model proposed by Yönaç et al [6] is studied. This model does not have stochastic noise fields like in the previous model and there is no coupling between the two cavities. Therefore, the evolution of the entanglement is a pure information-exchange evolution meaning there is no decoherence. Due to the non-existence of decoherence and studying in a single mode, the entanglement resurrects. If the atoms are entangled initially, the local atom-cavity couplings provide non-local entanglement between the cavities. Two groups of partially entangled Bell states are examined being $|\Phi\rangle$ and $|\Psi\rangle$ for different cavity initial states being one photon, more than one photon, coherent state, and mixed state. The concurrence results for both one and more than one photon cases are quite similar. The only difference is the frequency of the concurrence. Increasing the photon number increases the frequency due to the Rabi frequency G_n term, which depends on both the coupling constant and the number of photons. Whereas, for the coherent state cavity case, the magnitude of the concurrences shows exponential decay in general by changing the real part of the coherent state of the cavity. As a final different initial state in a single-mode cavity is a mixed state. This state consists of pure states $|\Phi\rangle$ and $|\Psi\rangle$ with different probabilities. For this initial state, the entanglement exchange between the different pairwise can be observed as well. As mentioned in [2, 6], entanglement sudden death occurs (ESD) for the $|\Phi\rangle$ state. Similarly, for the other initial state cases, in this work, it is found that ESD occurs. Changing the parameters such as the real part of the coherent state, the number of photons yields a change in the ESD time reciprocatively. Furthermore, the conservation relations are examined for different initial states. As given in [10], one can always find an entanglement conservation relation for $|\Psi\rangle$ state, which is also the case for this paper. The conservation relation for $|\Phi\rangle$ is found for one and more than one photon initial case. Finally, the effect of the mode number in the cavity is investigated. Yu and Eberly [4] stated that for the infinite-mode cavity, no rebirth of the entanglement happens after a finite time. Only, a small number of the cavity modes lead to entanglement resurrection. According to these results, one can expect an ESD time increase in the two-modes field. In this paper, the approach for the calculation is given; no numerical solution can be provided yet to observe the ESD time increase. As a later study, noisy channels used in Section II and double JC models in III can be combined for different initial states.

[1] Ting Yu and JH Eberly. Qubit disentanglement and decoherence via dephasing. *Physical Review B*, 68(16):165322, 2003.

[2] M Yönaç, Ting Yu, and JH Eberly. Pairwise concurrence dynamics: a four-qubit model. *Journal of Physics B: Atomic, Molecular and Optical Physics*, 40(9):S45, 2007.

[3] Peter W Shor. Scheme for reducing decoherence in quantum computer memory. *Physical review A*, 52(4):R2493, 1995.

[4] Ting Yu and JH Eberly. Finite-time disentanglement via spontaneous emission. *Physical Review Letters*, 93(14):140404, 2004.

[5] William K Wootters. Entanglement of formation of an arbitrary state of two qubits. *Physical Review Letters*, 80(10):2245, 1998.

[6] Muhammed Yönaç, Ting Yu, and JH Eberly. Sudden death of entanglement of two jaynes–cummings atoms. *Journal of Physics B: Atomic, Molecular and Optical Physics*, 39(15):S621, 2006.

[7] Gerard J. Milburn D.F. Walls. *Quantum Optics*. Springer Berlin, Heidelberg, 2008.

[8] Lecture 20: Cavity qed-the jaynes-cummings model from https://www.lkv.uni-rostock.de/storages/uni-rostock/Alle_MNF/Physik_Qms/Lehre_Scheel/quantenoptik/Quantenoptik-Vorlesung11.pdf.

[9] Ting Yu and JH Eberly. Sudden death of entanglement. *Science*, 323(5914):598–601, 2009.

[10] Stanley Chan, MD Reid, and Z Ficek. Conservation rules for entanglement transfer between qubits. *Journal of Physics B: Atomic, Molecular and Optical Physics*, 43(21):215505, 2010.